

**CHANGES IN STREAMBANK ERODIBILITY AND CRITICAL SHEAR
STRESS DUE TO SURFACE SUBAERIAL PROCESSES**

By Marc Bryson Henderson

**Thesis submitted to the Faculty of Virginia Polytechnic Institute and State University in
partial fulfillment of the requirements for the degree of
Master of Science
In
Biological Systems Engineering**

**Theresa Wynn (Co-Chair)
David Vaughan (Co-Chair)
Lucian Zelazny**

**May 11, 2006
Blacksburg, VA**

**Key Words: soil erodibility, critical shear stress, streambank erosion, soil desiccation,
freeze-thaw cycling**

Copyright 2006, Marc B. Henderson

CHANGES IN STREAMBANK ERODIBILITY AND CRITICAL SHEAR STRESS DUE TO SURFACE SUBAERIAL PROCESSES

By Marc Bryson Henderson

Abstract

Previous studies have shown that soil erodibility and critical shear stress are highly influenced by weathering processes such as freeze-thaw cycling and wet-dry cycling. Despite over forty years of research attributing changes in soil properties over time to climate-dependent variables, little quantitative information is available on the relationships between streambank erodibility and critical shear stress and environmental conditions and processes that enhance streambank erosion potential. The goal of this study was to investigate temporal changes in streambank erodibility and critical shear stress due to surface weathering.

Soil erodibility and critical shear stress were measured monthly *in situ* using a multi-angle submerged jet test device. Environmental and soil data were also collected directly at the streambank surface to determine freeze-thaw cycles, soil moisture, soil temperature, bulk density, soil erodibility, critical shear stress, and other atmospheric conditions that could impact bank erosion potential. Statistical tests, including a nonparametric alternative to ANOVA and multiple comparison tests, were used to determine if temporal changes in soil erosion potential were greater than spatial differences. Regression analyses were also utilized to identify the factors contributing to possible changes in soil erodibility, critical shear stress, and bulk density.

The nonparametric alternative to ANOVA in combination with Dunn's nonparametric multiple comparison test showed soil erodibility was significantly higher ($p=0.024$) during the winter (November - March) and the spring/fall (April - May, September - October). Regression analyses showed 70 percent of soil erodibility variance was attributed to freeze-thaw cycling alone. Study results also indicated that bulk density is highly influenced by climate changes since gravimetric water content and freeze-thaw cycles combined explain as much as 86 percent of the variance in bulk density measurements.

Results of this study show significant amounts of variation in the resistance of streambank soils to fluvial erosion can be attributed to subaerial processes, specifically changes in soil moisture and temperature. These results have potential implications for streambank modeling and restoration projects that assume constant values for soil erodibility. Watershed

models and restoration designs should consider the implications of changing soil erodibility during the year in model development and stream restoration designs.

Dedication

I would like to dedicate this work to my parents, Linda and Leon Henderson, whose lives and careers have set the ultimate example for me. Not only did they set a high standard for me, but their endless support enabled me to step outside of my comfort zone and be successful at Virginia Tech. For this support, I owe my parents more than words can describe. This work is more a reflection of their hard work in raising me to be the person that I am today than it is a reflection of my own abilities as a student.

Acknowledgements

I would like to thank my major professor, Dr. Tess Wynn, for all of her time, effort, ideas, experience, and endless support during my graduate studies. Without her encouragement and confidence in my ability to accomplish my goals, I would have never made it through such a life-changing experience. Had it not been for Dr. David Vaughan's phone call to invite me to spend a summer participating in undergraduate research with Dr. Wynn (she was just Tess back then), none of this work would have ever taken place. One application to a summer research program had the power to open the door for me to develop as a person and a professional. I will always be grateful to Dr. Vaughan for granting me my first opportunity to come to Virginia Tech.

I would like to thank Dr. Lucian Zelazny for sitting on my committee and contributing a lifetime of expertise to my research. I would like to thank Laura Teany, the one person who spent more days with me in the sun, cold, rain, and snow than anyone else during the course of my research. To say Laura simply helped me complete my research would be an understatement. Without you, I would have never made it through the first winter, let alone the following spring, summer, fall, and winter again. There were times when you were cold, hungry, and could not feel your toes but you never complained. I appreciate that. I would also like to thank Julie Jordan who welcomed me into her lab to process my soil samples and provided me with anything I asked even though she was under no obligation to do so. I would like to thank Dr. Greg Hanson with the USDA ARS Hydraulics Lab in Stillwater, OK for allowing me to borrow the jet test device to conduct my research.

I would also like to thank all of my fellow graduate students for contributing to such an unforgettable two years. Without all the friendships I developed during my brief term at Virginia Tech, my graduate experience would have fallen far short of my expectations. Thank you also to the handful of graduate and undergraduate students in the Biological Systems Engineering Department who contributed their time and effort to many long days of field work. Thank you to Brian Benham for hosting so many great Friday afternoon get-togethers. They will inevitably become some of my fondest memories from Tech.

Beyond all else, I would like to thank my friends and family back home who encouraged me to follow my heart when I decided to leave home to pursue my graduate education. Without

their support and understanding, I would not have been able to accomplishing my goals this far from home. The long list of sacrifices you made on my behalf will never be forgotten.

Table of Contents

Abstract	ii
Dedication	iv
Acknowledgements	v
List of Figures	viii
List of Tables	x
Chapter 1 Introduction	1
1.1 Goals and Objectives	4
Chapter 2 Literature Review	5
2.1 Freeze-Thaw Cycling	7
2.1.1 Soil Moisture	9
2.1.2 Soil Type	10
2.1.3 Soil Structure	12
2.2 Soil Wetting-Drying Processes	14
2.2.1 Soil Desiccation	14
2.2.2 Soil Moisture	14
2.2.3 Wet-Dry Cycling	15
2.2.4 Clay Mineralogy	15
2.3 Soil Mineralogy	17
Chapter 3 Methods Section	21
3.1 Field Methods	21
3.1.1 Study Location	21
3.1.2 Streambank Soil and Temperature Monitoring	24
3.1.3 Jet Tests	25
3.2 Data Post-Processing and Data Analysis	31
3.2.1 Data Post-Processing	31
3.2.2 Evaluating Temporal Variations in K_d and τ_c	32
3.2.3 Determining the Influence of Subaerial Processes on K_d and τ_c	34
Chapter 4 Results and Discussion	38
4.1 Seasonal Variability of K_d and τ_c	51
4.2 Weathering Influences on K_d and τ_c	59
Chapter 5 Conclusions	66
Chapter 6 References Cited	69
Appendix	75
Vita	82

List of Figures

Figure 1 Simple 2:1 layer silicate diagram (McBride, 1994).	17
Figure 2 Simple 1:1 layer silicate diagram (McBride, 1994).	17
Figure 3 Layer organization of kaolinite (McBride, 1994).....	18
Figure 4 Layer organization and water location of swelling Smectite layers. Dashed lines are representations of charge distribution (McBride, 1994).....	20
Figure 5 Layer organization of Vermiculite (McBride, 1994)	20
Figure 6 Structure of secondary mineral, Illite (McBride, 1994).	20
Figure 7 Structure of 2:1:1 layer silicate Chlorite (McBride, 1994).....	20
Figure 8 Location of Stroubles Creek Watershed in relation to the Town of Blacksburg, Montgomery County, and the State of Virginia, USA (Benham et al., 2003).....	23
Figure 9 Location of experimental reaches along Stroubles Creek, southwestern Virginia, USA.	24
Figure 10 View of TDR probe inserted into streambank.....	26
Figure 11 Jet tank, point gauge, and associated equipment.....	27
Figure 12 Cross-section of jet test while running.	29
Figure 13 Cross-section of jet test during scour depth reading.	29
Figure 14 Overall jet test setup.	29
Figure 15 Data processing diagram for cluster data development.....	33
Figure 16 Data processing flow chart.	35
Figure 17 Air temperature sensor data processing flow chart.	36
Figure 18 Monthly maximum and minimum actual and historical temperatures for the study time period for Blacksburg, VA, USA.....	39
Figure 19 Actual monthly precipitation totals during the study period and historical monthly precipitation totals from Blacksburg, VA, USA.....	40
Figure 20 Unpublished data from jet test evaluation study using remolded soil blocks of silt loam soil.....	42
Figure 21 Plot of soil erodibility versus critical shear stress from data collected between February 2005 and January 2006 on Stroubles Creek, VA, USA.....	43
Figure 22 Soil erodibility and critical shear stress scatter plot with power curve trendline for Stroubles Creek, near Blacksburg, VA.	44
Figure 23 Seasonal average monthly soil temperature for the period February 2005 through January 2006 along Stroubles Creek near Blacksburg, Virginia, USA.	46
Figure 24 Seasonal average monthly soil volumetric moisture content for the period February 2005 through January 2006 along Stroubles Creek near Blacksburg, Virginia, USA.....	47
Figure 25 Mean and maximum solar radiation values for February 2005 through January 2006 from Kentland Farm, Blacksburg, VA, USA.....	48
Figure 26 Box plot of soil erodibility (K_d) by month along Stroubles Creek near Blacksburg, Virginia, USA.	49
Figure 27 Box plot of critical shear stress (τ_c) by month along Stroubles Creek near Blacksburg, Virginia, USA.	50
Figure 28 Box plot of bulk density (BD) by month along Stroubles Creek near Blacksburg, Virginia, USA.	51

Figure 29 Monthly mean soil moisture content for banks along Stroubles Creek, near Blacksburg, Virginia, USA.....	53
Figure 30 Seasonal K_d values along Stroubles Creek near Blacksburg, Virginia, USA, with two winter outliers of 8.6 and 3.9 $\text{cm}^3/\text{N-s}$ were eliminated from the figure.	54
Figure 31 Seasonal τ_c values along Stroubles Creek near Blacksburg, Virginia, USA.....	55
Figure 32 Seasonal bulk density values along Stroubles Creek near Blacksburg, Virginia, USA,	56
Figure 33 Gravimetric Water Content by site along Stroubles Creek near Blacksburg, Virginia, USA.....	57
Figure 34 Seasonal monthly rainfall totals for the period February 2005 through January 2006 near Blacksburg, Virginia, USA.	58
Figure 35 Seasonal average monthly air temperature for the period February 2005 through January 2006 near Blacksburg, Virginia, USA.....	59
Figure 36 Freeze-thaw cycle count by month along Stroubles Creek near Blacksburg, Virginia, USA.....	61

List of Tables

Table 2.1 Characteristics of analyzed soil (Deneff et al., 2002.	16
Table 4.1 Descriptive statistics for soil erodibility and critical shear stress data sets during the study period on Stroubles Creek, VA, USA.	45
Table 4.2 Mineralogical analyses results for composite bank material taken from along Stroubles Creek near Blacksburg, VA, USA.	60
Table 4.3 Statistically significant regression equations.	65
Table A-1 Field data collected monthly during jet testing.	75
Table A-2 Monthly soil moisture and temperature data.	76
Table A-3 Number of freeze-thaw cycles three, 10 and 30 days prior to jet-test for each month using average soil temperatures.	78

Chapter 1 Introduction

Assessments performed by the Environmental Protection Agency (USEPA) as part of the National Water Quality Inventory: 2000 Report identified sedimentation as one of the most prevalent forms of pollution in our nation's rivers and streams (USEPA, 2000). Sediment impairments are associated with declines in aquatic life and habitat, such as the hindrance of fish reproduction, fish suffocation, increased water turbidity, and negative impacts on benthic invertebrates (Berry et al., 2003). Numerous studies have shown that channel erosion can contribute as much as 90 percent of total watershed sediment yield (Langendoen and Wells, 2004; Lawler et al., 1999; Trimble, 1997). While streambank erosion itself is a natural process and is not a cause for concern, excessive streambank erosion can contribute to bridge failures, loss of agricultural lands, downstream sedimentation, habitat loss, and flooding (Langendoen and Wells, 2004).

Streambank erosion and retreat are the function of numerous mechanisms working in concert to form what is casually referred to as the single process of "streambank erosion" (Lawler et al., 1997a). In reality, research has identified three main processes by which most "erosion" occurs (Couper and Maddock, 2001; Hooke, 1979; Lawler, 1992, 1995; Lawler et al., 1997a; Wynn and Mostaghimi, 2006b). Specific definitions of these processes used from this point forward were adapted from definitions proposed by Lawler et al. (1997b). Erosion is the detachment, entrainment, and removal of particles or aggregates from the streambank surface. Fluvial and subaerial processes are typically recognized as the main contributors to streambank erosion as it is being defined in this study. Subaerial processes are commonly recognized as the wetting, drying, freezing, and thawing of surface soil, which leads to an overall weakening of the soil surface, as well as erosion (Couper and Maddock, 2001). Fluvial processes are the result of hydraulic forces applied directly to the streambank by flowing water. Mass failure of a streambank takes place when geotechnical instability causes a portion or all of a streambank to collapse or fail. Streambank retreat is the collective loss of bank material due to subaerial processes, fluvial entrainment and mass failure processes (Lawler et al., 1997a). This study focuses in particular on the tendency for subaerial processes to weaken the soil surface rather than quantifying physical amounts of erosion caused by these forces.

Subaerial processes as a whole have been characterized as “preparatory” processes that aid fluvial entrainment by loosening soil particles and aggregates at the bank face (Couper and Maddock, 2001). These processes are the result of changing climatic conditions that affect the soil moisture quantity, state, or movement within streambank soils (Thorne, 1982). Subaerial processes have been subdivided into three main categories based on soil moisture conditions. Lawler et al. (1997b) classified these categories as prewetting, desiccation, and freeze-thaw. Pre-wetting incorporates the mechanisms that increase the soil streambank moisture content. These mechanisms can include prolonged high flows, groundwater rise, and infiltration of precipitation (Lawler et al., 1997b). Desiccation of the bank surface leads to soil cracking and exfoliation (Lawler et al., 1997b). Freeze-thaw processes occur in streambank soils due to the freezing of soil moisture during cold nights and subsequent thawing during warmer daytime temperatures. Lawler et al. (1997b) suggested that for cohesive bank material, the processes that most influence streambank erodibility are subaerial processes.

Once the streambank soils are weakened, they are more susceptible to erosion by fluvial entrainment. Fluvial entrainment is defined as the removal of soil particles or aggregates from a channel by hydraulic forces (Thorne, 1982). Shear stresses develop at the interface of the flowing stream and the stationary streambank due to the differences between the velocities of these two media. This difference then creates drag forces which detach and entrain aggregates. When the soil particles are held loosely at the soil surface, more soil scour is likely to occur. Studies by Lawler (1993), Prosser et al. (2000), and Simon et al. (1999) showed significant increases in erosion following subaerial processes (Couper and Maddock, 2001). Fluvial entrainment at the bank toe then leads to mass failure and the direct deposit of large amounts of soil into the stream.

Hanson and Cook (2004) utilized the following form of the excess shear stress equation to determine erosion rates, ϵ_r (m/s):

$$\epsilon_r = K_d(\tau_e - \tau_c) \quad (1)$$

where K_d ($m^3/N\cdot s$) is the soil erodibility, τ_c (N/m^2) is the critical shear stress, and τ_e (N/m^2) is the effective stress. Soil erodibility is a soil property that quantitatively describes the erosion potential of a particular soil. According to Van Klaveren (1998), shear stress is the force produced by flowing water on a channel’s bed or sides in the direction of flow. Erosion begins

when a minimum amount of shear stress is reached to cause particle removal from the sides of a channel. Critical shear stress is the shear stress threshold at which hydraulic forces will begin to remove significant amounts of bank material. The effective stress is the actual stress applied to a streambank by a given flow. If effective shear stresses exceed the critical shear stress of a soil, erosion will occur. Any shear stress less than the critical shear stress should hypothetically not remove soil particles from a channel. At smaller stresses, particle entrainment may still occur due to turbulent fluctuations in the flow (Van Klaveren, 1998). Often, when the values of soil erodibility and critical shear stress are applied in a watershed model, average values of K_d and τ_c are chosen to represent the soil characteristics of large stream reaches (Allen et al., 1999). In contrast to this typical practice, research by Wynn and Mostaghimi (2006a) indicated both K_d and τ_c were influenced by subaerial processes, suggesting these parameters may vary seasonally. Studies have also shown that spatial variation in K_d and τ_c can vary by up to four and six orders of magnitude, respectively (Hanson and Cook, 2004).

Models such as SHE, WEPP, and SWAT use forms of the critical shear stress equations for determining overland erosion rates for rill, interrill, and channel erosion (Byne, 1999; Wynn, 2004). Byne (1999) used the critical shear stress equations from WEPP to develop new rill and interrill subroutines for ANSWERS-2000 and to add a channel scour subroutine as well. Soil erodibility coefficients are also inputs for HEC-6 (reach-scale hydraulics model), SWAT (basin-scale hydraulic model), and a bank/bed stability model developed by Osman and Thorne (1988) (Allen et al., 1999; Arnold et al., 1998; USACE, 1993; Wynn, 2004). CONCEPTS, a channel evolution model used to simulate open-channel hydraulics, sediment transport, and channel morphology, relies on the critical shear stress method for calculations of fluvial erosion rates (Langendoen, 2000).

Bank retreat is a complicated process due to significant spatial and temporal variability in soil erodibility; therefore, additional research is needed to identify the mechanisms which control soil erodibility (Lawler, 1992). While research on spatial variability in streambank erodibility has been addressed (Hanson and Cook, 2004; Wynn, 2004), little is known about temporal changes. Among the factors that vary temporally are freeze-thaw, desiccation, and bank moisture processes. Further research is needed to determine whether there are significant variations in K_d and τ_c over time and what role subaerial processes may play in these variations.

1.1 Goals and Objectives

The overall goal of this research was to investigate temporal changes in streambank erodibility and critical shear stress due to surface weathering. The specific objectives were to:

1. Determine the significance of temporal variability in streambank critical shear stress and erodibility; and,
2. Evaluate the influence of surface weathering by subaerial processes on streambank critical shear stress and soil erodibility.

Chapter 2 Literature Review

Streambank retreat is influenced by a variety of factors that include fluvial geomorphology, bank hydrology, location of a stream reach within a watershed, and bank structural characteristics (Lawler, 1992; Lawler et al., 1997b). The varying temporal and spatial scales of streambank retreat makes identifying the specific causes of retreat difficult. Often, multiple processes are at work and cannot be separated. This complexity has made research into individual bank retreat mechanisms important. Lawler (1992) developed a set of process groups to categorize the different mechanisms involved in streambank retreat. These groupings, as described by Lawler (1992), are weakening processes, direct fluid entrainment, and mass failure. The most commonly described and researched weakening processes are pre-wetting of the bank surface, desiccation, and freeze-thaw activity (Lawler et al., 1997b). These processes are also referred to collectively as subaerial processes.

Studies by Wolman (1959) and Twidale (1964) were some of the first studies to note significant influences of subaerial processes on bank retreat. The degree to which each author attributed their observed and recorded streambank retreat to subaerial processes varied. Wolman (1959) found both wet conditions and frost activities had significant effects on streambank retreat. Between 1953 and 1958, Wolman monitored erosion on two cross-sections of Watts Branch in Rockville, MD. Using erosion pins and surveying techniques, Wolman recorded changes in the channel cross section. The erosion pin measurements indicated the winter months from December to March produced the most bank retreat from the two sites. He also noted that 85 percent of the measured bank retreat occurred during winter months, the time in which the mechanisms of pre-wetting and frost action occurred. Wolman (1959) compared climatic data to the retreat record to determine any correlations. When compared, the retreat record revealed the scenario of high flows occurring after “thoroughly wet” conditions yielded higher retreat rates than just high flows alone. During the summer months, Wolman recorded no significant instances of retreat even though the largest flood of the study period occurred during July of 1956. This storm event illustrated that high flows were not able to cause as much retreat as the high stage events coupled with saturated banks. Previous saturation of the bank material was necessary to cause significant bank retreat. This observation is noteworthy because it was one of the first clear illustrations of the important role climatic conditions have on bank retreat.

In the same study, Wolman (1959) also cataloged events that indicated freeze/thaw processes alone played a role in bank retreat events. One of the observations made during the study was that increased stage height following freezing temperatures provided conditions that encouraged bank material removal. Wolman noted that bank toe material was loosened by frost action and was subsequently removed by an increased water level. This study also recorded increased stage heights that did not produce bank toe removal. The author linked this lack of erosion to the lack of frost action prior to the stage increase.

This work by Wolman (1959) directly led to more work on the subject of river bank erosion by Twidale (1964). In Twidale's study, erosion pins were used to quantify bank retreat at four sites on the Torrens River, Adelaide, France. Rainfall data were directly correlated with the bank retreat observed over the two-year study period. Some incidents of retreat were often delayed or did not coincide with peak flows, while other instances revealed that high flows were the cause of the retreat. Twidale noted that bank material remained at the toe of the bank after it was removed from the bank surface. This observation indicated the material had been deposited following the peak event; otherwise, the material would have been removed or altered by the peak stream flows. At other times during the two year study, material was not found at the toe of the bank. These observations indicated multiple processes were contributing to the bank retreat on the Torrens River.

Knighton (1973) conducted an observational study over the course of 18 months to evaluate causes and mechanisms of streambank retreat along the River Bollin-Dean, in Cheshire, UK. Bank retreat was tracked using erosion pins and periodic cross-sectional surveys. Knighton reported in his study that as much as 70 percent of all erosion occurred as a result of high discharge levels. Subaerial processes were observed to prepare banks for large amounts of soil removal during high flows. Cracks caused by both freeze-thaw and wet-dry processes contributed to the efficiency with which the high discharges removed soil from the banks of the Bollin-Dean. Most freeze-thaw effects reported by Knighton followed the previously mentioned role of subaerial processes as being strictly preparatory for future fluvial entrainment. Weakening of bank material and disaggregating the bank surface soil were the main observable affects of frost action.

Hooke (1979) examined relationships between bank retreat and hydrologic and climatic data using multiple linear regression. Retreat rates were measured along multiple river segments

in Devon, England using erosion pin sets spaced in 2- to 3-m intervals horizontally. Each set of pins consisted of pins inserted into the bank to form a vertical line up the streambank with 30-cm spacing between each pin. Hooke found soil moisture provided the highest statistical explanation of the measured bank retreat. The study also showed that different variables dominated along different stretches of river. Areas of river bank with less cohesive soils showed positive correlation between high soil moisture and bank retreat. On river reaches where more cohesive soils were present, both high moisture content and high flows were correlated with increased retreat rates. Negligible erosion was measured when cohesive river banks were dry.

2.1 Freeze-Thaw Cycling

Seasonal differences in climate and weather conditions can play a major role in bank retreat rates. Studies by Wolman (1959), Thorne and Lewin (1979), Hooke (1979), and Twidale (1964) all showed a majority of retreat events occurred during winter months when the channel banks were wetter and more susceptible to fluvial erosion from high flows. Wolman (1959) estimated that 85 percent of erosion occurred during the winter months of December and March. The direct deposition of soil into Watts Branch was observed as a result of soil previously incorporated within ice crystals being subsequently released following soil thawing. When this freeze-thaw process took place, a rise in stage was not needed for the contribution of sediment to the stream to take place. This release of soil from ice crystals is an example of subaerial erosion as an erosion mechanism and not simply a preparatory process.

A varying climate can impact streambank soils in several different ways. First, the excessive freeze-thaw cycling of soil moisture is a destructive process. While initial freeze-thaw cycles (0 to 4 cycles) can increase surface aggregate stability (Lehrsch, 1998), larger numbers of cycles have been shown to reduce surface aggregate stability (Edwards, 1991; Lehrsch et al., 1991; Mostaghimi et al., 1988). This decrease in soil aggregate stability increases erosion (Wynn et al., 2004).

Frozen soil pore water can also weaken banks by reducing cohesive forces and intergranular interlocking (Thorne, 1982). Several authors have noted that soils with silt-clay contents above 20 percent show increased frost susceptibility (Couper and Maddock, 2001).

Freeze-thaw processes are caused by the freezing and subsequent thawing of soil moisture in streambank soils. When the atmospheric conditions reduce the temperature at a bank face, both hydraulic gradients and freezing occur. A strong relationship exists within soil between temperature and pressure. Pore pressures within a soil can drive water movement from one location within the soil to another. When a soil freezes, the soil matric potential is proportional to the temperature decline below 0°C within the soil. The matric potential is the soil water suction created by capillary and adsorptive forces within the soil structure. The hydraulic potential created by a temperature gradient of only 1 K/m can provide enough suction to create 120 meters of water pressure head per meter of soil. As water is drawn towards the freezing front where the low temperatures are present, the soil moisture content in this area is increased. The increase in soil moisture can cause weakening of the soil structure. The increase in moisture can also provide greater expansion of the soil as the water at the freezing front freezes and expands. This expansion causes frost action, which is the strain created by the expansion of frozen soil (Craig, 1992).

Like classic early studies conducted by Wolman (1959), Twidale (1964), and Knighton (1973), Lawler (1986) showed a correlation between frost activity and streambank retreat. Lawler's study took place on two meander bends on the Ilston River, Gower, UK. On these bends, Lawler installed a system of erosion pins. The pin network consisted of four to eight pins arranged in a vertical line with each line being set 1-m apart horizontally along the streambank. A total of 230 pins were installed between March 1977 and January 1978 and were read monthly from March 1977 until June 1979. Three gauging stations collected continuous flow data in close proximity to the pin networks. Lawler collected temperature, rainfall, and soil moisture data a few kilometers from the erosion sites at the nearby Penmaen meteorological station. From these data, strong statistical correlations between air frost and erosion rates were developed. The specific definition Lawler used for air frost in his statistical analysis was the percentage of days with air frost (minimum air temperature at or below 0° C) in the erosion period. Lawler also reported that stream flow and ground-frost showed "very strong" correlation and were also statistically significant variables at $\alpha = 0.05$. Rainfall and antecedent wetness showed weaker correlation while still being statistically significant variables. Ultimately, frost action in combination with bank wetting was the most significant predictor variable in this specific study.

Observations made by Lawler (1986) illustrated why freeze-thaw processes have the potential to play such a large role in bank retreat. Lawler observed that bank material prepared by needle ice growth was quite erodible when contacted by high stream stage. When stream stage increased beyond the influence of needle ice growth, only the material impacted by the frost action was entrained. This observation showed that the bank material by itself was not highly susceptible to erosion, but that the freeze-thaw action reduced soil strength, which then increased fluvial entrainment.

One of the main freeze-thaw forms observed and reported in the literature is needle ice. Needle ice is small diameter ice crystals that extend perpendicular to the direction at which the bank loses heat to cold night air (Lawler et al., 1997b). Soil particles are often incorporated as ice crystals develop on the streambank surface (Hanson, 1996; Lawler et al., 1997b). As the needle ice melts during warmer daytime temperatures, this entrapped sediment is released and can move either lower on the bank or directly into the stream (Lawler et al., 1997b). The bank surface becomes disturbed and is easily eroded with the next rise in stream stage (Lawler, 1987, 1993).

2.1.1 Soil Moisture

Soil moisture content at the time of freezing influences the impact of freeze-thaw cycling. Branson et al. (1996) investigated the conditions under which needle ice formed in 139 laboratory experiments on undisturbed soil samples taken directly from a river bank where needle ice had been observed in the past. The grain size distribution for this soil was 11 percent clay, 46 percent silt, 42 percent sand, and 1 percent gravel. Branson et al. (1996) placed the samples in topless acrylic sample containers designed to provide constant moisture to the samples. To prevent freezing from the bottom, the bottom of the sample was insulated and a slight heat flux consistent with what is found in a natural environment due to ground heat flux was applied to the sample bottom. The block face that had been exposed previously to stream flow and atmospheric conditions on the river bank was placed face-up in the open face of the box. Soil moisture and temperature readings were taken at multiple depths below the soil surface. Soil heave at the surface was also measured with a linear displacement transducer. During the experiment, one data set was collected with varying cooling curves and constant soil moisture, while another data set was collected with a constant cooling curve and variable soil

moisture. After the completion of each experiment on a sample, the needle ice was evaluated for length of needles and mapped for overall coverage on the soil surface.

Branson et al. (1996) found that as the temperature dropped below 0°C, moisture moved towards the freezing front of the soil sample. The moisture content one cm below the surface increased while the soil temperature never reached 0°C. As the temperature dropped below freezing and the moisture moved through the soil towards the freezing front, clear needle ice formed at the soil surface. Soil inclusion in the ice occurred when either the temperature or moisture fluctuated. When a sudden temperature drop occurred and the moisture moving to the freezing front could not keep up, the freezing front descended further below the surface. If the moisture flow then increased and reached equilibrium with the temperature, needle ice began to form behind the first band of frozen soil. Sediment was pushed toward the surface as a layer of soil and ice ahead of the forming needle ice. This included soil is exposed to potentially erosive conditions such as high flows or thawing of the needle ice. From these results, Branson et al. (1996) concluded soil moisture and temperature control how and when needle ice will form. Soil inclusion into needle ice only occurred if the equilibrium between the heat energy loss from the soil surface and soil moisture supply to the freezing front was disrupted. These conclusions were made under the assumption that hydraulic conductivity was not a limiting factor in the movement of soil moisture towards the freezing front. Soil moisture was the most important factor in soil inclusion during needle ice formation: if moisture did not move towards the freezing front fast enough to produce needle ice, the freezing front descended into the soil profile. The formation of needle ice could only resume if soil moisture was available in a quantity that returns system equilibrium.

2.1.2 Soil Type

The streambank soil type plays an important role in the susceptibility of soil to freezing processes. Finer-grained sediments allow the movement of moisture to the freezing front, increasing soil moisture at the bank surface and the likelihood of needle ice formation (Couper, 2003). The pores in silt-size materials are large enough to maintain the flow of soil moisture through the bank to the freezing front while still small enough to allow for capillary rise. Fine-grained materials such as clays do not permit rapid moisture movement while coarse-grained materials do not provide sufficient capillary rise to relocate water higher in the bank profile

(Ferrick and Gatto, 2005). Matsuoka (1996) identified a minimum silt-clay content of 20 percent for soils to be frost susceptible.

Couper (2003) evaluated the impact of silt-clay content on the susceptibility of river banks to subaerial erosion using laboratory experiments to replicate freeze-thaw cycles on soil samples with varying silt-clay contents. Both “undisturbed” and remolded soil samples were tested. Remolded soils with silt-clay contents of 30-75 percent were created to match the averages of the silt-clay contents of the field samples. Soil blocks, 1500 mm x 900 mm x 600 mm, were placed in 1-m x 1-m plastic container and then subjected to either humidity cycling or freeze-thaw cycling. For the humidity cycling, soil samples were exposed to 70, 24-h humidity cycles with a range of 68-90 percent. Freeze-thaw cycling was simulated by 28 24-h cycles of -6°C for 10 h and 6°C for 14 h. Dimensions of the soil blocks were recorded after every cycle and any eroded material from the one exposed surface was collected and analyzed for total dry mass and aggregate size. Couper (2003) observed a greater occurrence of erosion and large-aggregate formation from the high silt-clay samples during the 28 freeze-thaw cycles than with lower silt-clay samples. Higher silt-clay soils produced a larger amount of eroded material at silt-clay contents above 50 percent. The other measured variable, aggregate size, also increased considerably as silt-clay content exceeded 50 percent of the soil. Study results indicated a statistically significant correlation coefficient (r) of 0.778 between silt-clay content and the mass of eroded material from the samples.

In a laboratory study, Ferrick and Gatto (2005) evaluated how a single freeze-thaw event impacted the erosion of a silt soil. The laboratory study used bins of pre-formed Hanover silt at similar bulk densities to investigate rill erosion caused by a concentrated flow of clear water down pre-made, rectangular, longitudinal rills. These initial rills were made by tamping the soil surface with an 8-cm wide steel plate to the depth of 1.5 cm below the soil surface. Three series of experiments were conducted using low moisture content (16-18 percent by volume), medium moisture content (27-30 percent by volume), and high moisture content (37-40 percent by volume) soils. The soil samples were frozen and thawed at -35°C and 25°C, respectively, using a freezing plate on the soil surface. Each soil tray was frozen through its entire depth and completely thawed for only one cycle before the experiments took place. Freezing time varied from sample to sample depending on soil moisture content. The thawing of each soil sample lasted between 27 and 45 h. The total mass of soil eroded from each bin was measured and

compared to erosion from an unfrozen control. The study showed a significant increase in sediment yield from the bins which experienced the one freeze-thaw cycle. Sediment load ratios reported from this study showed two to four times as much sediment was eroded from the low and medium moisture freeze-thaw samples as compared to the unfrozen control bins. Up to 12.7 times as much sediment loss occurred in the high-moisture freeze-thaw samples than in the unfrozen control samples. While this study did not compare different soil textural classes, it did confirm that for a silt soil, even one freeze-thaw can increase sediment loss from the soil.

In the Western Cape mountains of South Africa, Boelhouwers (1998) investigated the climatic and material properties that influence soil frost processes. Two field sites were equipped with stratified soil moisture sensors, stratified soil temperature sensors, air temperature sensors, and tipping bucket rain gauges. Data were recorded for the Waaihoek Peak site from January 1990 until December 1994. For the Mount Superior site, data recording started on May 1993 and commenced in December 1994. Both soil material and frost conditions varied between the sites: the Waaihoek site was composed of a shallow sandy soil with a thickness of 0.35 m while the Mount Superior site contained a 0.15-m thick sandy loam. The Mount Superior site regularly exhibited visual evidence of frost-susceptibility in the form of “active soil-frost processes” while the Waaihoek site did not show any signs of soil-frost processes (Boelhouwers, 1998).

Boelhouwers (1998) found the Waaihoek site did not demonstrate a propensity for “frost-induced soil processes” even though an average of 74 frost days a year occurred at this location. Moisture regimes and freezing temperatures favorable to freeze-thaw events were present at both sites; the significant difference between the two sites was particle size. The sandy soil of Waaihoek had 4-5 percent fines while the sandy loam of Mt. Superior had 24 percent fines. Boelhouwers (1998) concluded soil texture was the major factor limiting observable needle ice formation at the Waaihoek site.

2.1.3 Soil Structure

Soil structure influences soil properties such as porosity, infiltration, aeration, and drainage (Denef et al., 2002; Six et al., 2000). Aggregate stability is frequently used as a proxy for measuring soil structure (Six et al., 2000). Aggregate stability is a quantitative measure of a soil aggregate’s ability to withstand forces which tend to breakdown its structure (Lehrsch and

Brown, 1995). These disruptive forces may include physical or climactic stresses such as wetting, drying, freeze-thaw, or water erosion (Denef et al., 2002; Lehrs and Brown, 1995). Multiple studies have been conducted to determine the factors that influence aggregate stability. Oztas and Fayetorbay (2003) investigated the effects of freeze-thaw cycling on a series of samples with different physical and chemical properties from the Erzurum Province of Turkey. The soil samples were air dried and sieved into three aggregate size classes. The samples were then brought up to one of three moisture contents (air dry, field capacity, and 90 percent saturation) and then frozen at either -4 or -18°C. Freezing conditions were maintained for 24 hours and followed by 24-hrs at 5°C. These cycles were repeated 3, 6, and 9 times. Three aggregate size classes (0-1, 1-2, 2-4 mm), four parent materials, three freeze-thaw cycles, three moisture contents, and two different freezing temperatures were tested. Treatment effects were determined by an Analysis of Variance and Duncan's multiple comparison test was used for a comparison of means.

Even though freeze-thaw cycling lowered the initial wet aggregate stability of every soil tested, the results showed that soil structure played a critical role in freeze-thaw susceptibility. Soils with a higher initial aggregate stability were more affected by the freeze-thaw cycling. Of the four soils tested, the Tuzcu had the poorest structure (lowest initial aggregate stability) and had the lowest percent change in aggregate stability. To contrast, the Pasinier soil had an average aggregate stability reduction from 72 percent to 34.8 percent after freezing and thawing. The Pasinier soil began the test with a higher aggregate stability than the Tuzcu soil. The difference in results for the two different soils shows that a low aggregate stability is impacted less by freeze-thaw cycling than a high aggregate stability. The researchers also found aggregate stability decreased with increased soil moisture; indicating the aggregates were less likely to remain stable if they were frozen at an approximately saturated state (Oztas and Fayetorbay, 2003). Study results also showed aggregate stability increased from 3 to 6 cycles, but then declined from 6 to 9 cycles.

One limitation with using aggregate stability as a surrogate for erosion potential is that changes in aggregate stability cannot be directly related to the potential erosion of a cohesive streambank (Couper, 2003). While aggregates may decrease in size when exposed to freeze-thaw cycles, the tests derived to measure these losses were not developed in the context of streambank erosion (Couper, 2003). This limitation makes applying their results directly to a

streambank erosion application difficult. More research is needed to see if changes in aggregate stability are related to streambank retreat.

Studies of the effect of freeze-thaw processes on aggregate stability have provided mixed results. As reported by Asare et al. (1997), some studies indicated improved soil structure following freeze-thaw cycling, while some other studies reported the opposite result. At the conclusion of their own study, Asare et al. (1997) found a decrease in surface shear strength as freeze-thaw cycles increased. Lehrsch (1995) found that aggregate stability increased with the first two freeze-thaw cycles, but was not affected by freeze-thaw cycling after the second freeze-thaw cycle. Mostaghimi et al. (1988) found aggregate stability decreased strikingly between the third and sixth freeze-thaw cycle. Because aggregate stability is seen as a control of erosion, preventing freeze-thaw cycling can reduce soil losses from erosion (Oztas and Fayetorbay, 2003).

2.2 Soil Wetting-Drying Processes

2.2.1 Soil Desiccation

According to work by both Kemper and Rosenau (1984) and Schahabi and Schwertmann (1970) drying a soil can increase strength and structure (Denef et al., 2002). Soil drying increases the “intermolecular associations between organic molecules and mineral surfaces (Kemper and Rosenau, 1984) and the sorption of oxides on clay domain surfaces (Schahabi and Schwertmann, 1970)” (Denef et al., 2002). Drying of a soil can also strengthen the soil structure through the precipitation of cement and bonding agents or by arranging clay particles between those of sand and silt (Lehrsch, 1998).

2.2.2 Soil Moisture

Denef et al. (2002) stated that slaking is one way in which a stable dry soil is transformed into a wet, less stable soil. Slaking is the process by which soil disintegrates under rapid wetting (Lado et al., 2004). Factors contributing to slaking include the escape of confined air from within soil, differential swelling of soil, the rapid release of heat during wetting, and the physical movement of water over soil aggregates (Lado et al., 2004).

At the other extreme, high soil moisture tends to lessen the interparticle forces within soil (Craig, 1992). Moving water within the bank can lead to a softening of the bank or the removal

of soil particles by suspension or solution (leaching) (Thorne, 1982). Once soil cohesion is disrupted, soil becomes more vulnerable to high stream flows and the fluvial entrainment that follows.

2.2.3 Wet-Dry Cycling

Wet-dry cycling can lead to both beneficial and destructive phenomena. Low soil moisture can lead to cracks in the outermost surface of a streambank (Dietrich and Gallinatti, 1991; Osman, 1988; Thorne and Lewin, 1979). These cracks are referred to as desiccation cracks. According to Thorne (1990), the desiccation cracks between soil peds act as planes of weakness where the soil blocks between cracks are stronger than the soil forces holding the peds together. Drying processes are commonly viewed as preparatory processes (Couper, 2003). Desiccation cracks loosen the soil and peds on a bank face and make it readily available for removal by fluvial entrainment. Streambanks are increasingly susceptible to wetting and drying processes due to changes in stream stage. Rising stream stage provides the hydraulic forces necessary for fluvial entrainment to take place. These rises in stream stage are most notable in urban streams or low order streams due to the streams' rapid rise during and immediately after storm events and the "flashy" nature of their hydrographs.

2.2.4 Clay Mineralogy

In laboratory experiments, Deneff et al. (2002) collected three different soils samples from areas used for long term agricultural research. Characteristics of these three soils are listed in Table 2.1. The soil samples were processed by air drying for two days and then passed through a 250 μm sieve to break up all macroaggregates. Larger sand and particulate organic matter fractions were added back into the sample following sieving. The moisture content of the three different sets of soil samples was brought up to field capacity (21 and 27 g $\text{H}_2\text{O}/100$ g of air-dried soil).

Table 2.1 Characteristics of analyzed soil (Denef et al., 2002).

Soil Sample Location	Weathering Characteristics	Mineralogy
Article I. Sidney, NE	Lightly weathered, temperate soil	<ul style="list-style-type: none">• 2:1 clay minerals (illite and chlorite)
Lexington, KY	Moderately weathered soil	<ul style="list-style-type: none">• 2:1 and 1:1 clays (vermiculites and kaolinites)• amorphous and poorly crystalline oxides
Passo Fundo, Brazil	Highly weathered soil	<ul style="list-style-type: none">• 1:1 clays (kaolinites)• High number of Fe- and Al-sesquioxides

The three different soils were exposed to two separate treatments of either fast drying followed by slow wetting or slow drying followed by slow wetting. At 14-day intervals, the fast dry samples were removed from jars and exposed to 25°C temperatures and dried to 1-2 percent moisture in two days. The soils were then rewetted slowly to field capacity. For the slow drying, the samples were constantly exposed to a drying environment and then water was added when the samples reached 50 percent of field capacity moisture content by weight. These samples were also slowly brought to field capacity. Analysis of the aggregate size and stability was conducted using both a wet-sieve method for “unstable” aggregation and a wet-sieve procedure using an air-dried sample to determine “stable” aggregation. At the conclusion of the experiment, Denef et al. (2002) observed that the wetting and drying of a soil increased “unstable” macroaggregate formation in the three soil samples being studied for both dry-wet treatments. Differences between dry-wet treatments were only observed with the 2:1 soil from Sidney, NE. The author proposed that the differences between soils developed from a higher sand fraction in the 2:1 soil. The higher sand fraction caused a more intense reaction to the rewetting during the fast dry- slow wetting treatment. A second hypothesis for the different reactions of the 2:1 soil to the different dry-wet treatments is the presence Fe and Al oxides. The Fe and Al oxides in the 2:1 soil may have strengthened the soil aggregates enough during the faster drying treatment to resist degradation (Denef et al., 2002).

2.3 Soil Mineralogy

Clay minerals occur in natural landscapes in many forms but the most stable and persistent forms of silicates fall into the category of sheet silicates (McBride, 1994). Layer silicate clays are arranged in many different forms because of the varying arrangements of tetrahedral silicate sheet and octahedrally coordinated metal cations. A 1:1 layer silicate such as kaolinite would have a one layer tetrahedral silica sheet paired with an octahedral sheet filled with metal cations such as aluminum or magnesium or possibly a combination of both (McBride, 1994). An alternate structure for layer silicates is the mica structure which is composed of two tetrahedral sheets of silica on either side of one octahedrally coordinated cation sheet (McBride, 1994). The formation is typically referred to as a 2:1 layer silicate because of the ratio of tetrahedral sheets to octahedral sheets.

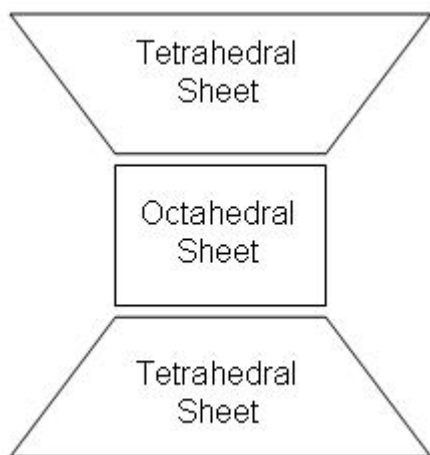


Figure 1 Simple 2:1 layer silicate diagram (McBride, 1994).

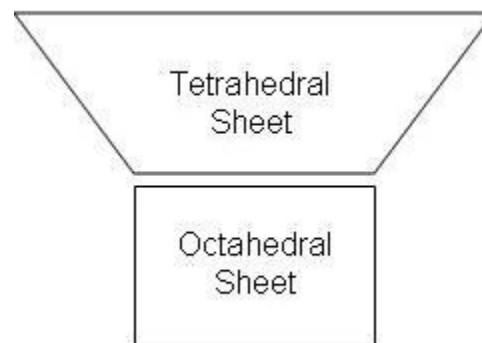


Figure 2 Simple 1:1 layer silicate diagram (McBride, 1994).

Clay mineralogy plays a key role in controlling the formation and stabilization of aggregates (Denef et al., 2002). In the previously mentioned experiment, control soil samples were stored for the same 42 days as the treatment soil samples. When analyzed, the controls showed an increase in aggregation that depended on the soil mineralogy. The 1:1 soil had greater aggregation than the mixed soil, while both 1:1 and the mixed soil had greater aggregation than the 2:1 soil. Previous research has shown that a soil, such as the 1:1 soil with high levels of charged mineral particles in the form of positively charged oxides and negatively

charged 1:1 clay minerals, shows an increased ability to form both micro and macro-aggregates due to the electrostatic interactions developed from the clay minerals of differing charge (Denef et al., 2002). In contrast, 2:1 soils contain mineral particles of similar negative charge which are bound by positively charged metal cations to the negatively charged surface of soil organic matter. This allows 1:1 soils to form aggregates independent of soil organic matter (SOM) unlike 2:1 soils which depend heavily on SOM to form aggregates (Denef et al., 2002).

Bank material type has a strong impact on whether desiccation produces soil cracking; the extent of shrinking and swelling within the soil depends directly on the clay mineral type and content of the streambank material (Couper, 2003). As the soil plasticity increases with fine particle content, so does the propensity for shrinking and swelling effects of silt-clay soils due to moisture fluctuations (Couper, 2003). The reaction of different clay minerals to environmental conditions is a function of the molecular structure of the clay. One common 1:1 layer silicate, kaolinite, has been found to not swell when saturated by water (McBride, 1994). This lack of swelling occurs because the structure has no charge and is strongly bonded by OH^- groups and O^{2-} ions on either side of the two sheets. Two layers of kaolinite are represented in Figure 3.

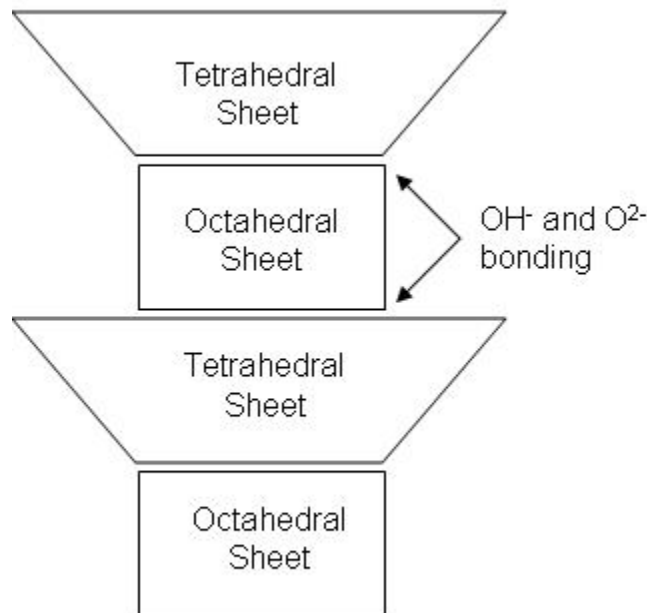


Figure 3 Layer organization of kaolinite (McBride, 1994).

Smectites are 2:1 layer silicates which include isomorphic substitution within their octahedral or tetrahedral layers (McBride, 1994). Smectites are known for their low layer charges which allow the layers to part and make way for water particles to enter between layers. The ease in layer separation is what causes smectites to swell in the presence of water. Smectite is seen in Figure 4. Vermiculites are similar to smectites in structure but have a greater layer charge than smectites. This means that vermiculite will not swell as much as smectites because of more limited layer expansion (McBride, 1994). Charge is often the only distinguishing characteristic between smectites and vermiculites (McBride, 1994). A diagram of vermiculite's structure is found in Figure 5. Illites are secondary minerals characterized by a 2:1 silicate, mica-like structure but still retains potassium (K^+) between its silicate layers (McBride, 1994). A diagram of this layer silicate is found in Figure 6. This trapping of K^+ prevents the layers from expanding to accept water molecules. Because of this, Illite is unable to swell in the presence of water. Chlorite belongs to a separate mineral group from the micas and the 1:1 layer silicates. Chlorite is known as a 2:1:1 layer silicate. A diagram of the layered structure of chlorites is found in Figure 7. Between the tetrahedral and octahedral layers lies a positively charged metal hydroxyl sheet which acts to stabilize the sheets against changes in soil moisture content. McBride (1994) notes that the lack of an aqueous sheet between layers allows chlorite to never dehydrate or swell in response to varying moisture regimes. Dehydration is the process by which a mineral will lose surface water (H_2O) but not structural OH^- .

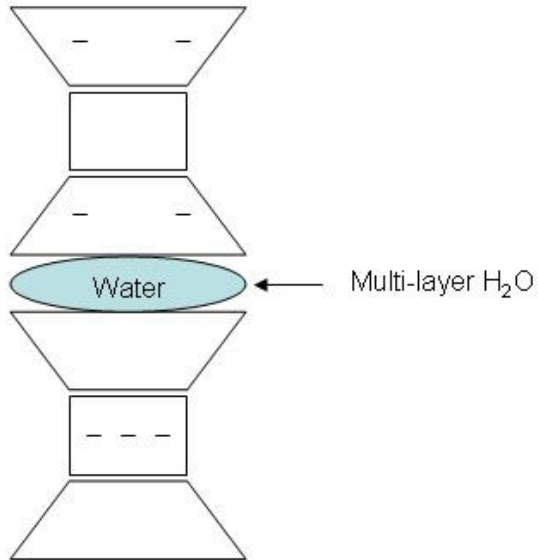


Figure 4 Layer organization and water location of swelling Smectite layers. Dashed lines are representations of charge distribution (McBride, 1994).

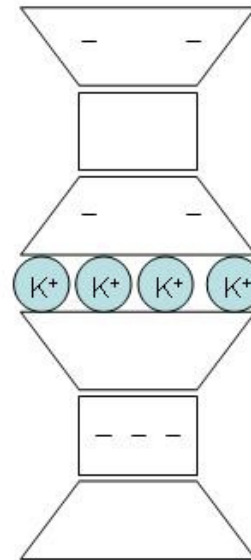


Figure 6 Structure of secondary mineral, Illite (McBride, 1994).

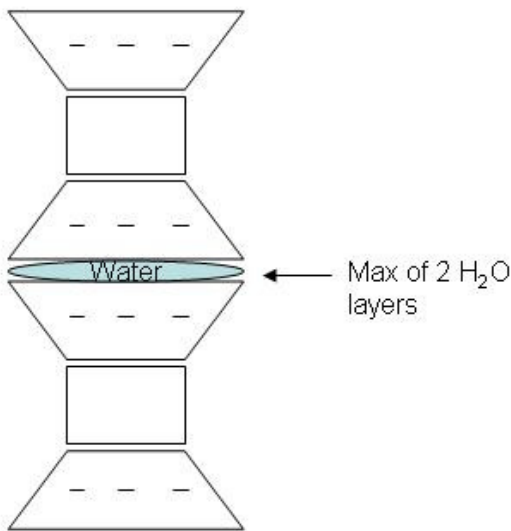


Figure 5 Layer organization of Vermiculite (McBride, 1994) .

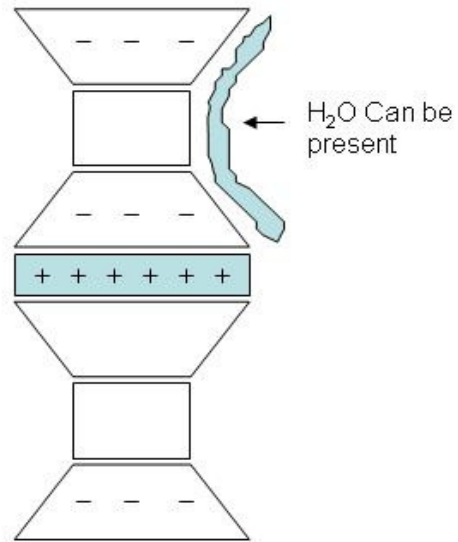


Figure 7 Structure of 2:1:1 layer silicate Chlorite (McBride, 1994).

Depending on clay mineralogy, different mechanisms can control binding of aggregates. In 2:1 clay minerals, polyvalent metals, and polyvalent metal-organic matter complexes are primarily responsible for creating linkages between negatively charged 2:1 clay particles (Six et al., 2000). Organic matter complexes play less of a role in binding due to a lack of organic

matter lower in the soil profile. Iron and aluminum oxides and 1:1 clay mineral particles are the primary bonding agents that create stability within the soils when these soil attributes are dominant (Six et al., 2000). Six et al. (2000) cited the electrostatic interactions between the oxides and the 1:1 clay minerals as the reason behind a reduction in the impact of SOM to increase aggregation.

The presence of clay has been shown to increase soil cohesion and prevent aggregate destruction under various stresses (Kemper et al., 1987). Kemper et al. (1987) contended that soil strength is highly influenced by the frequency and duration of past exposures to moisture. Rapid wetting of a soil surface drives air from pore spaces and disrupts interparticle bonds between microaggregates within larger aggregates. In previous work, Kemper et al. (1985) found that the threshold for aggregate damage by air displacement was 0.30 kg/kg of initial water content. After full wetting occurs, clays particles move into suspension and are deactivated as bonding agents due to reduced contact with larger particles (Kemper et al., 1987). This contact between clay particles and larger particles or microaggregates is a significant mechanism in the bonding of soil. As soils dry, these clay particles become lodged next to larger particles and aggregates and again strengthen the soil. Precipitates then form at these clay-microaggregate binding sites and further strengthen these bonds. Because mineral to mineral contact is required for soil cohesion, increased water content weakens contact between minerals. Water molecules adhere to the mineral surfaces through interactions with diffuse layer cations and act as a buffer between minerals. Soil drying brings the minerals closer due to an increase in water tension. When these minerals move closer to each other, they then are put in contact with each other and form bonds.

Chapter 3 Methods Section

3.1 Field Methods

3.1.1 Study Location

Study sites for this research were located within the Stroubles Creek watershed, which is located within Montgomery County, Virginia as pictured in Figure 8. The Stroubles Creek watershed is located in southwestern Virginia, USA within the Ridge and Valley Level III Ecoregion, and the Limestone/Dolomite Valleys and Low Rolling Hills Level IV Ecoregion of

the Appalachian Mountains (Benham et al., 2003). The Town of Blacksburg (37° 14'N, 80° 25'W) has a temperate climate with a historical average annual rainfall of 1029 mm distributed uniformly throughout the year (SERCC, 2005). The historical annual average temperature is 10.6°C, with annual average maximum and minimum temperatures of 17.3° and 4.4°C, respectively (SERCC, 2005). A diagram of the Stroubles Creek research area is shown in Figure 9. In this figure, the colored lines indicate jet test site locations and the monitoring equipment site. This reach of Stroubles Creek is a second order, gravel-bed stream with an 8 km² drainage area that receives surface water contributions from both the Town of Blacksburg and the Virginia Tech campus. The study reach is located in a pasture that is actively grazed by dairy cattle and has active streambank retreat taking place. Average baseflow water level is 20 cm with bank heights of 1.0-1.3 m. This location was chosen due to observations of needle-ice formation and desiccation cracking made during previous studies along Stroubles Creek (Wynn and Mostaghimi, 2006b). The floodplain soils are McGary (Fine, mixed, active, mesic Aeric Epiaqualfs) with 60 cm of silt loam overlying 40-50 cm of loam.

Sites were selected to have the approximate aspect of 130 degrees from magnetic north and shear, unvegetated banks, as previous research has shown streambank aspect and roots density influence soil erodibility (Wynn and Mostaghimi, 2006b). The selected sites were measured and marked at their upstream and downstream boundaries by wooden stakes. The lengths of the experimental reaches ranged from 10 m to 18 m. Following site selection, failed soil blocks were removed from the toe of the streambank to expose the entire bank face to surface weathering. This work was completed two weeks before jet testing began to provide time for surface weathering to occur. All sites began the experiment period in the same condition with shear banks and no on-bank vegetation.

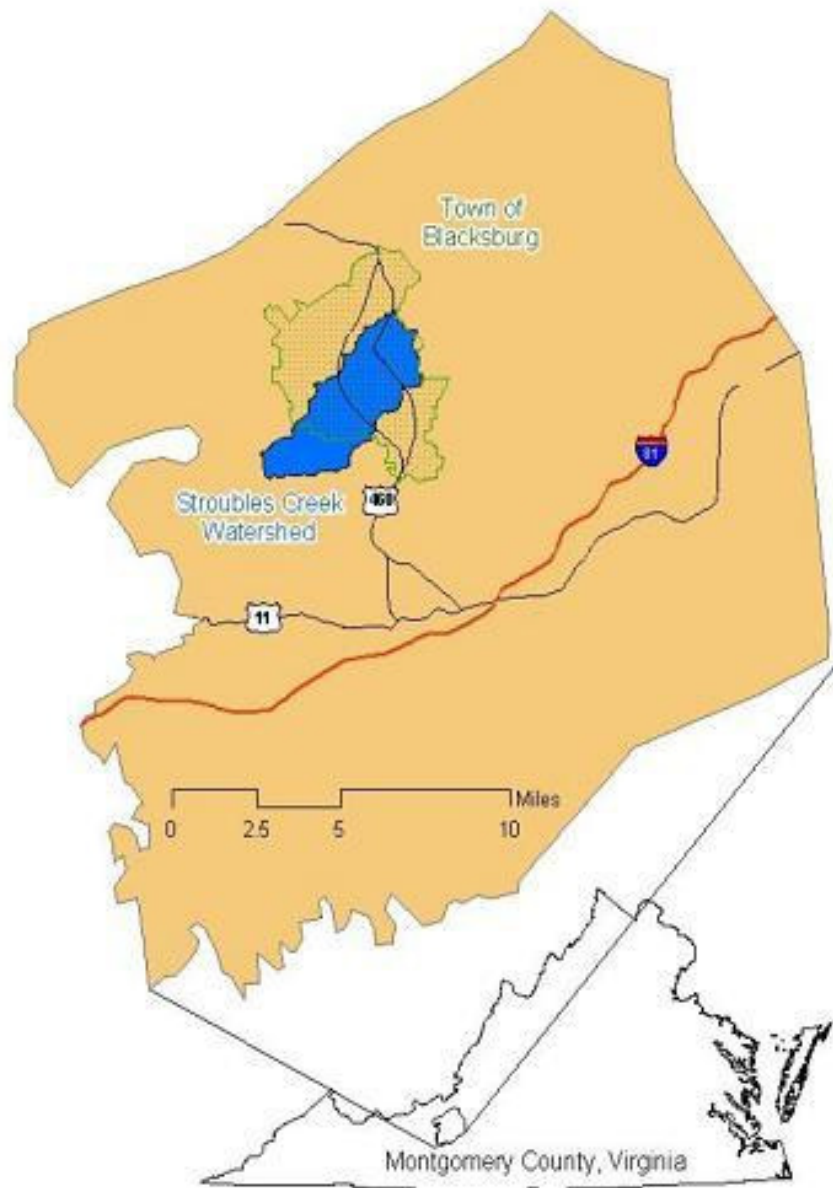


Figure 8 Location of Stroubles Creek Watershed in relation to the Town of Blacksburg, Montgomery County, and the State of Virginia, USA (Benham et al., 2003).



Figure 9 Location of experimental reaches along Stroubles Creek, southwestern Virginia, USA.

3.1.2 Streambank Soil and Temperature Monitoring

To evaluate changes in soil volumetric moisture content and temperature over time, one of the seven sites was chosen for year-round monitoring. A site located approximately in the middle of the study reach was designated to have soil moisture and soil temperature sensors installed directly into the bank face.

In January of 2005, ten Campbell Scientific 107-L temperature sensors (accuracy of $< \pm 0.5^{\circ}\text{C}$ for temperatures -35°C to $+50^{\circ}\text{C}$ and $< \pm 0.1^{\circ}\text{C}$ for temperatures -24°C to $+48^{\circ}\text{C}$) and ten Campbell Scientific CS605/610-L TDR probes (maximum soil bulk electrical conductivity of 1.4 dS/m) were installed in a 20-m section of streambank and monitored for 13 months. The twenty sensors were wired to a Campbell Scientific CR10X datalogger, with the TDR probes being routed through two SDMX50-series multiplexers and a Campbell Scientific TDR100 time-domain reflectometer. The equipment setup was powered by a sealed 12-volt battery. The Campbell Scientific 107-L temperature sensors were wired directly into the CR10X datalogger. All electrical equipment was placed within a Vynckier VJ-type enclosure UL listed per UL Standard 508 for NEMA 3, 3R, 4, 4X, 12 and 13. The ten pairs of probes were installed 1.5 m apart on a section of streambank between Site 3 and Site 4. The TDR probes were inserted horizontally into the bank 30 cm above the water level so that the metal tines of the probe were completely covered in soil. The probes were inserted as shallowly into the bank as possible while still completely covering them with soil. An installed TDR probe is shown in Figure 10. The temperature probes were placed in close proximity to the TDR probes, but care was taken to not place the temperature sensors where they may interfere with the TDR readings. An eleventh temperature sensor was left under the electronics enclosure out of direct solar radiation to monitor air temperature. Soil volumetric moisture content and temperature readings were taken every 30 minutes from Jan 13, 2005 to Jan 21, 2006. As a result of animal disturbance and sensor malfunction, three sensors were replaced during the study.

Precipitation was measured on site using a tipping bucket rain gauge, while stream stage was measured at an on site stream gauge. During periods of time when the rain gauge was not operational due to maintenance, rainfall data were replaced by one of two other rain gauges within the same rain gauge network. All three rain gauges were located within 5 km of each other within the Stroubles Creek watershed.

3.1.3 Jet Tests

Six submerged jet tests (one per site) were conducted monthly within the study reach from Feb 11, 2005 to Jan 21, 2006 to determine the streambank soil erodibility (K_d) and critical shear stress (τ_c). Each site was sampled within the same timeframe (2-3 days) to limit drastic weather changes between the six monthly tests.



Figure 10 View of TDR probe inserted into streambank.

A multi-angle submerged jet test device was used to measure K_d and τ_c in situ (ASTM, 1999; Hanson, 1997). The jet test device consisted of a submergence tank, jet tube, point gauge, head tank, several lengths of hose, and a pump as seen in Figure 11. The submergence tank was a 30.5-cm diameter steel ring that provided the base for the jet test apparatus. A removable Plexiglas lid that included a hinged door for access mounted to the submergence tank. The jet tube was made of two concentric Plexiglas cylinders inserted in the center of the submergence tank lid normal to the lid surface. The point gauge attached to the jet tube on the opposite side of the nozzle. The point gauge was used to both measure the depth of scour and to stop the jet test. The center cylinder of the jet tube stabilized the point gauge while it was attached to the jet tube. An adjustable head tank was used to supply water for the jet while maintaining a constant fluid

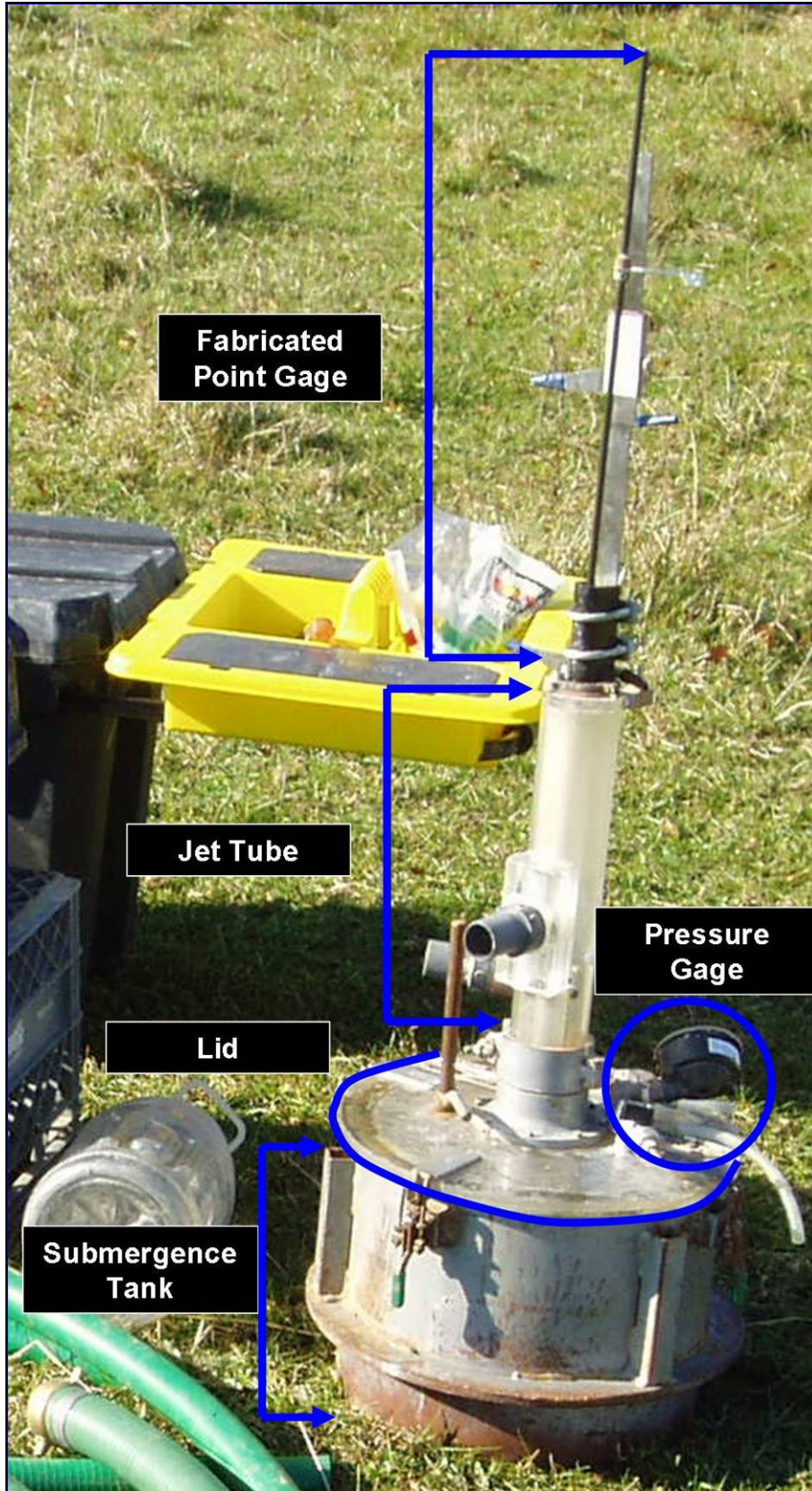


Figure 11 Jet tank, point gauge, and associated equipment.

pressure. The pressure change across the nozzle was measured on either side of the jet nozzle by an Ashcroft low pressure diaphragm gauge. The pump used for this research was a Honda WX15 portable pump.

The testing process began when the pump was started and water was transferred from the stream to the head tank (Figure 14). Constant pressure was maintained by the head tank with a small stand pipe attached to an overflow hose. This setup maintained a constant water level at the top of the head tank. The head tank then dispensed water through a hose into the jet tube which is pictured in Figure 11. The submergence tank was gently filled with water using a 2-l bottle and a siphon hose (Figure 11). Once the jet tube and submergence tank were full, the point gauge was removed from the 6.35-mm diameter orifice to begin bank scouring (Figure 12). A jet of water was then projected normally towards the bank, creating the scour for the jet test measurements. Excess water was removed via an overflow hose. The point gauge was moved in and out of the orifice (Figure 12 and Figure 13) to stop and start the test. A close-up image of the point gauge is found in Figure 11.

Prior to testing, initial benchmarks were recorded to determine the distance from the soil surface to the nozzle of the jet tube, which established distances from which all other point gauge measurements were compared. At five-minute intervals, high pressure and low pressure readings were recorded. Throughout the test high pressure readings were taken from the inside of the jet tube and low pressure measurements were taken from inside the submergence tank. Point gauge readings were taken coinciding with the pressure measurements. The water jet was stopped by sliding the point gauge through the jet nozzle (Figure 13). The diameter of the point gauge rod is the same as the nozzle diameter, thus preventing water from flowing from the jet tube to the submergence tank during scour depth measurement. The point of the rod was then slid to the soil surface and a scour depth reading was taken. This procedure was repeated every five minutes for 45 minutes.

Each month, one location was tested at each of the six sites on the study reach. The testing location was determined using a stratified random method. The first several months of testing required multiple attempted tests at many of the sites to achieve a complete 45-minute test, due to bank failures and blowouts around the submergence tank. Test locations were occasionally shifted from the first randomly selected number to the next number on the list due

to the presence of muskrat holes, damage from a previous test or soil sample, obvious vertical crayfish burrows, or interference from deposits of a recent mass failure.

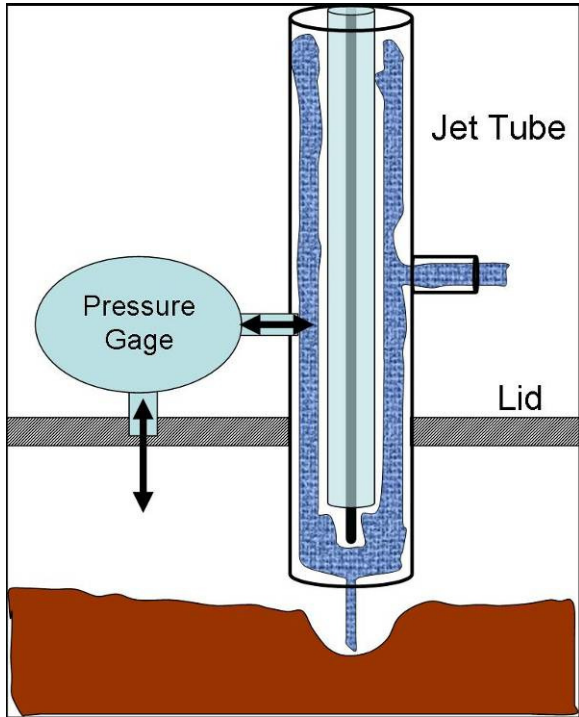


Figure 12 Cross-section of jet test while running.

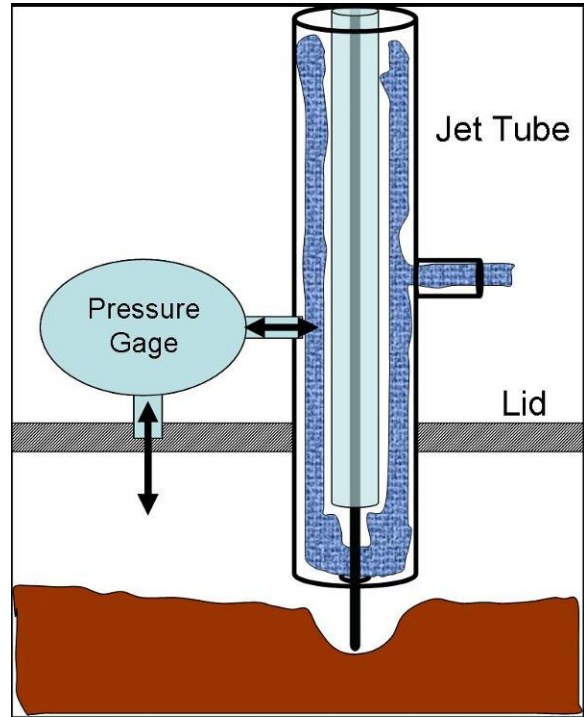


Figure 13 Cross-section of jet test during scour depth reading.

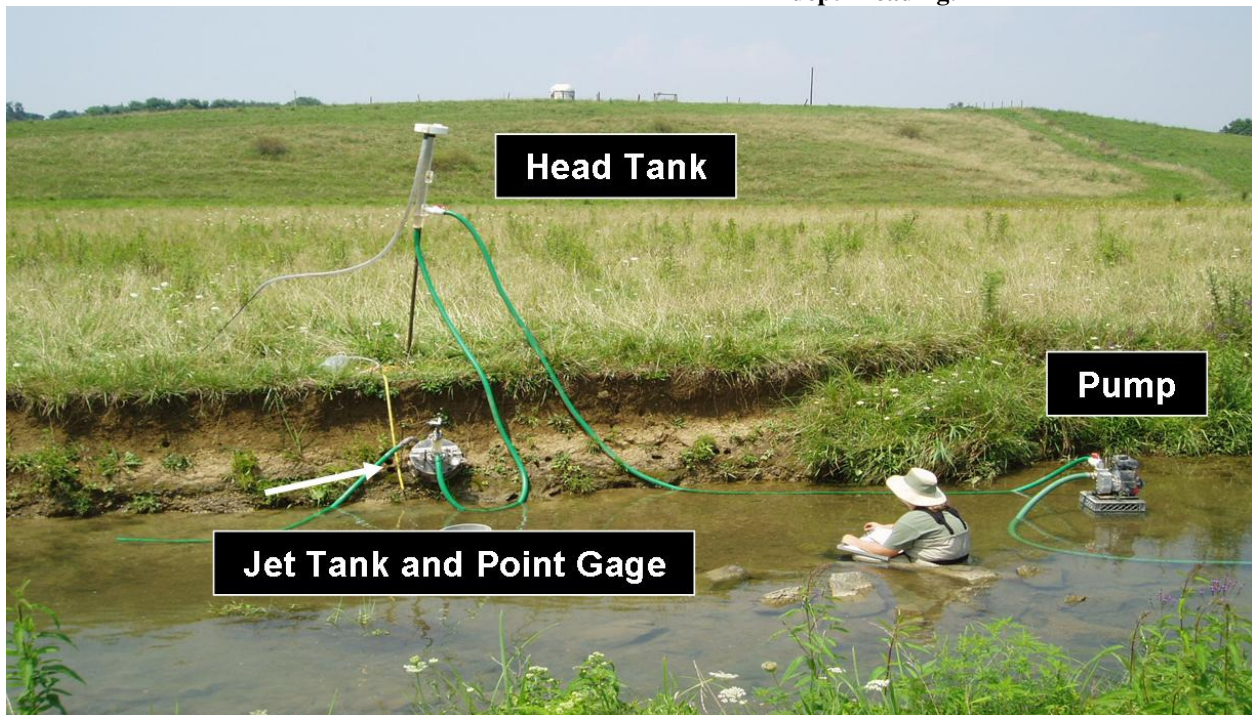


Figure 14 Overall jet test setup.

Care was taken to minimize disturbance of the test area while driving the submergence tank into the streambank to its maximum depth of 7.6 cm. The inside of the submergence tank was sealed at the soil/tank interface using bentonite to prevent piping of water under the tank. Bentonite was also used to seal any other spots around the submergence tank where a possible weakness was noticed. An example of a weakness is soft soil, a slight hole, or any other anomaly in the soil that could cause a water leak from the tank during testing. While setting up the jet tube, the distance from the nozzle orifice and the bank surface was set at approximately 7.5 cm. Hanson and Cook (2004) advised the distance between the orifice and the streambank surface be set anywhere between 6 and 32 nozzle diameters, with 12 nozzle diameters as the recommended setting.

Initial measurements were taken to determine benchmarks for the point gauge readings. Point gauge measurements were recorded with the tip of the point gauge flush with the nozzle orifice and with the tip of the point gauge at the surface of the bank. The initial point gauge reading at the surface of the bank established the datum from which all subsequent scour measurements were compared. To measure the actual head of the jet, the pressure on either side of the nozzle orifice was measured using an Ashcroft low pressure diaphragm pressure gauge. Pressure readings were measured at the four-minute mark of each test interval, which allowed enough time before the scour depth measurement to record both the high and low pressures. Once five minutes had passed, the jet was stopped by sliding the point gauge through the jet orifice. The door on the submergence tank cover was opened and the point gauge was guided by hand to the bank surface and the scour depth was measured. Measurements were continued until 45 minutes has passed and 9 depth recordings were made.

Data measured by the *in situ* testing of the streambank was entered into a spreadsheet routine developed by Hanson and Cook (2004) and processed through several pre-developed worksheets to calculate K_d and τ_c . The spreadsheet routine determines τ_c through the use of the scour depth vs. time data determined from the jet test device and a hyperbolic function developed by Blaisdell et al. (1981) for determining the final depth of scour (Hanson and Cook, 2004). Critical shear stress was then solved using the equilibrium depth found from the hyperbolic function. Soil erodibility was found by using the measured scour depth, time, the newly determined τ_c , and a dimensionless time function (Hanson and Cook, 2004). According to

Hanson and Cook (2004), the spreadsheet “minimizes the sum of deviations in the value of measured time based on observed test values and functionally determined values.” This calculation was done by fitting the data to the excess shear stress equation using a least squares method which yields soil erodibility.

Soil samples were taken prior to each jet test at the bank surface to determine both bulk density and gravimetric moisture content at each site. Pre-weighed 4.9-cm x 2.5-cm bulk density rings were used for each site. Soil samples were wrapped in plastic wrap, placed in labeled plastic bags and brought back to the Biological Systems Engineering Land and Water Resources Lab. The samples were placed in a 105°C oven for a minimum of 24 hours. The samples were then removed and allowed to cool inside a desiccation chamber before weighing.

One 300 cm³ composite soil sample was also created from soil taken from each of the six jet test sites to determine clay mineralogy of the streambank soils. The soil sample was air dried and sieved through a #10 test sieve (2-mm mesh) to remove all gravel from the samples. The mineralogical analysis consisted of x-ray diffraction and thermogravimetric analysis on the clay fraction of the soil sample (< 2 µm) (Zelazny, 2006). A pretreatment consisting of 30 percent H₂O₂ was used to drive off all organic matter. The sand fraction of the sample was removed by sieving and the clay and silt particles were separated through centrifugation and subsequent decantation of the clay fraction. X-ray diffraction was used to determine the various clay mineral components of the original bulk soil sample. Several samples of potassium-saturated and glycerol-solvated samples were examine using a Scintag XDS 2000 X-ray Diffractometer (Scintag, Santa Clara, CA) as both heated and non-heated samples. The potassium saturated sample was also analyzed using the thermogravimetric analyses using a Hi-Res TGA 2950 Thermogravimetric Analyzer (TA Instruments, New Castle, DE). Standards were run against the composite sample to identify specific X-ray diffraction peaks which were used to differentiate different clay minerals.

3.2 Data Post-Processing and Data Analysis

3.2.1 Data Post-Processing

Air temperature, soil temperature, and volumetric water content (VMC) data were collected every 30 minutes from January 13, 2005 until January 21, 2006. These data were checked for irregularities following download from the data logger. Irregularities usually

consisted of readings that were outside the bounds of realistic measurements. For soil moisture, this range was every reading of VWC less than 0.1 and greater than 0.6. This range was selected to conservatively eliminate any unreasonable data based on the typical range of observed data. Soil temperature was visually checked for large irregularities between any of the ten sensors that could indicate a faulty sensor. This error was most often characterized by long periods of extreme temperatures that were physically unrealistic, such as temperatures of $\sim 50^{\circ}\text{C}$ for a week or longer. Air temperature data were not eliminated because there was only a single air temperature sensor and the readings appeared reasonable. Once a complete data set was developed and errors were removed, the median of both the ten soil temperature and ten soil moisture sensor values was calculated at each time step. Using the median of the data removed the influence of individual extreme sensor values that would have otherwise skewed a calculation of the average. The median calculation yielded data sets of 30-minute soil temperature and soil moisture data that were used to create weathering parameters.

3.2.2 Evaluating Temporal Variations in K_d and τ_c

To determine if temporal variations in K_d and τ_c were statistically significant, cluster analysis was applied to weather-based data sets to separate the study months into seasonal groups. These groups were then analyzed for seasonal differences in soil erodibility and critical shear stress, using the Kruskal-Wallis nonparametric alternative to ANOVA.

Monthly values for air temperature, soil temperature, soil moisture, and precipitation were determined from the 30-minute data of air temperature, soil temperature, and volumetric water content. Precipitation was summed for each month to yield the monthly rainfall data set. For all data sets except precipitation, the monthly average of daily mean, maximum, and minimum values were calculated. Because soil moisture and soil temperature data were gathered from multiple sensors, the median value from the ten sensors was used to create the daily values. A visual representation of this process is found in Figure 15.

Months were grouped into seasons using the K-Observations function in MINITAB[®] and six different groups of soil and weather parameters. The groups were then used to create two, three, and four clusters using the six sets of data. Clusters were formed based on centroid linkages and Euclidean distance measures (Minitab, 2003). This analysis created 18 different clusters.

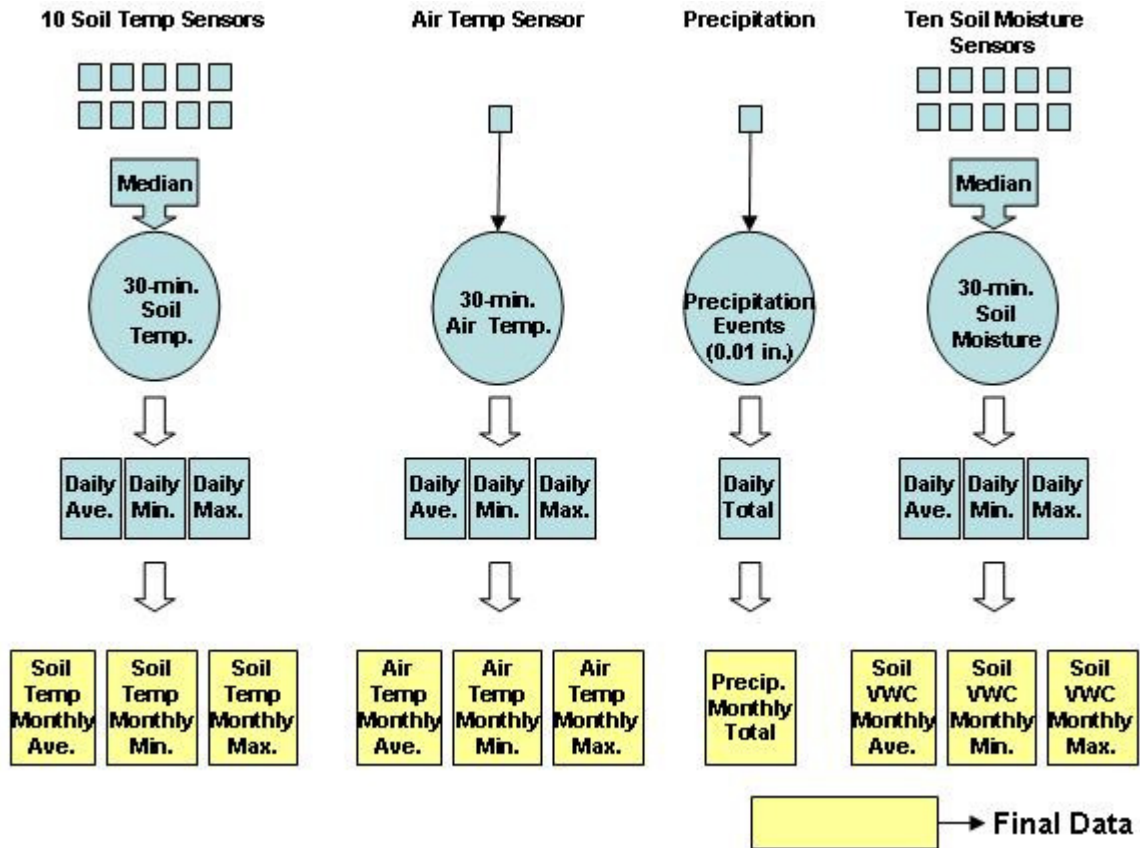


Figure 15 Data processing diagram for cluster data development.

A Kruskal-Wallis test was then run to determine if significant differences in K_d and τ_c existed between the seasonal groups. A non-parametric test was chosen because box plots of the data showed outliers and right-skewed distributions for all of the factor groupings. The Kruskal-Wallis test is a non-parametric analysis of the equality of means between two or more groups of data that has increased power for the analysis of non-normal data and outliers (Minitab, 2003). A statistical significance level of $\alpha = 0.05$ was used during the analysis to either except or reject the research hypothesis. The test having factor groupings with the lowest p-value was selected and evaluated for specific differences amongst grouping using a multiple comparison test. The research and null hypotheses were as follows:

$$H_0: \text{The seasonal distributions of } K_d \text{ and } \tau_c \text{ are identical.}$$

H_a : Not all the distributions are the same.

A Dunn Test was then performed to determine differences in seasonal K_d and τ_c populations (Zar, 1999). The Dunn Test is a nonparametric multiple comparison test that compares mean ranks to expand upon information already received from the Kruskal-Wallis test by identify which groups have statistically significant differences. This test is specifically intended for non-parametric multiple comparisons where sample sizes are unequal (Zar, 1999).

3.2.3 Determining the Influence of Subaerial Processes on K_d and τ_c

The second goal of the data analysis was to evaluate the influence of surface weathering by subaerial processes on streambank critical shear stress and soil erodibility. The most significant weathering parameters were determined using regression analysis. The independent variables for the regression analysis included summations of soil temperature, soil moisture, air temperature, stream stage, and number freeze-thaw cycles, while critical shear stress, soil erodibility, and soil bulk density were the dependent variables for the analysis.

The data sets of 30-minute air temperature, soil temperature, soil moisture, and maximum daily stage were used to create parameters representing conditions immediately prior to jet testing. Weather parameter means were calculated for the time period three days prior, 10 days prior, and 30 days prior to jet testing. The data processing progression for these data sets is visually represented in Figure 16. The 30-minute air temperature data were also used to create seven other weather parameter data sets. These data sets included overall maximum and minimum monthly air temperatures, mean daily maximum and minimum air temperatures, and monthly maximum, minimum, and average daily mean temperature. The processes used to develop these data sets are represented in Figure 16 and Figure 17.

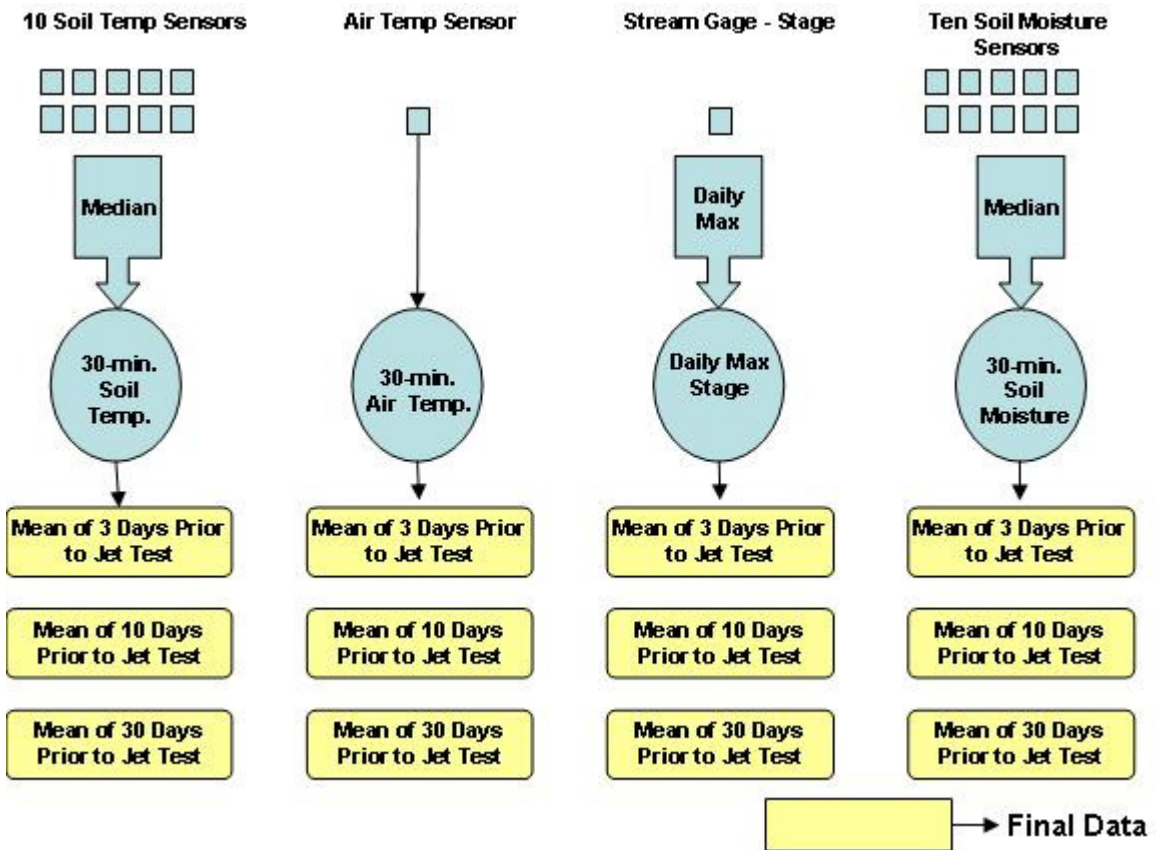


Figure 16 Data processing flow chart.

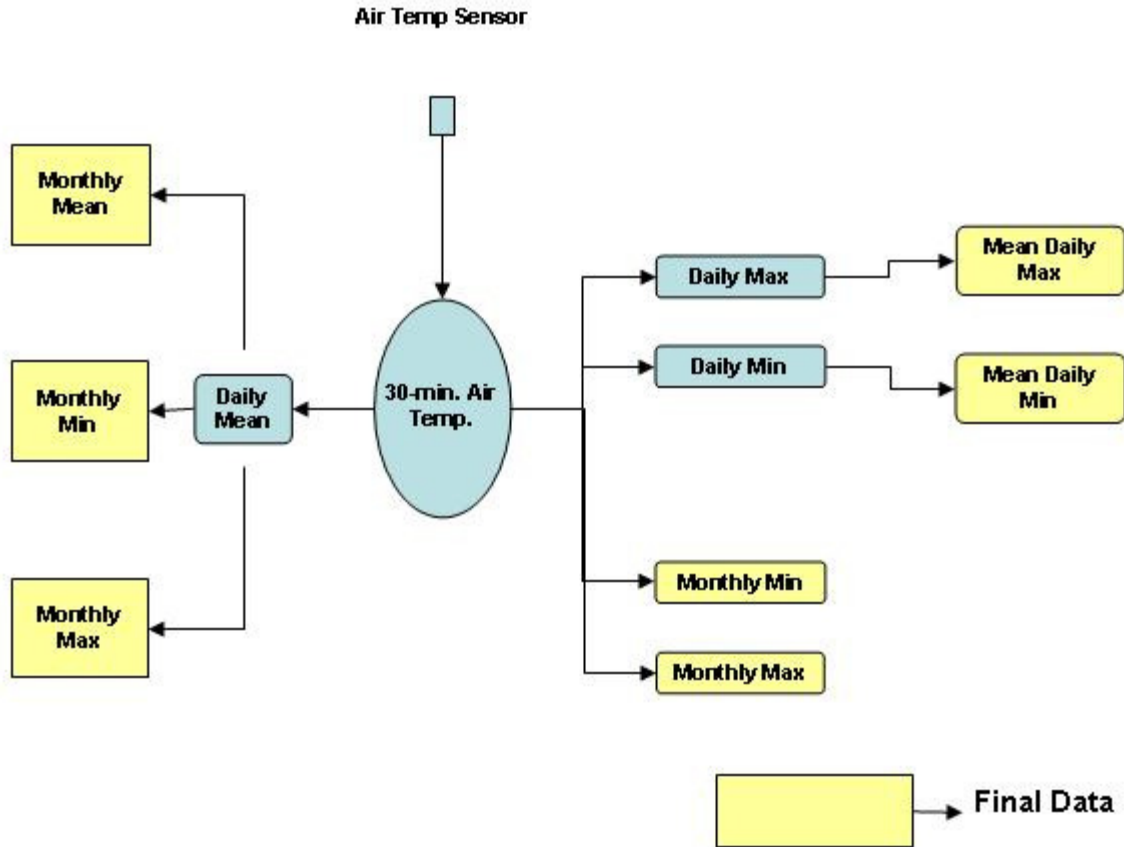


Figure 17 Air temperature sensor data processing flow chart.

The number of freeze-thaw cycles occurring during a given time period was determined by setting a temperature cutoff at which freezing and thawing could have occurred. This hypothetical cutoff was necessary because soil in a natural setting does not necessarily freeze at 0°C because of varying salt concentrations in the soil pore water (Branson et al., 1996). Several different freezing thresholds were used as a cutoff for freeze-thaw activity to compensate for the unknown effects of soil salinity, possible insulating affects of the soil overlying the temperature sensors, and any possible temperature sensor error. The number of freeze-thaw cycles was calculated using temperature cutoffs of 0°, 0.2°C, 0.5°C, 0.75°C, and 1.0°C to indicate “freezing”. These cutoff values were applied to the 10-sensor average, median, minimum, and maximum values for each time step. When temperatures changed from a “freezing value” to a non-freezing value, a freeze-thaw cycle occurred. Each change from a freezing condition to a thawed condition was summed for three time intervals prior to each monthly jet-testing. These intervals were 3 days prior, 10 days prior, and 30 days prior to jet-testing.

To determine the influence of climate on soil erodibility and critical shear stress, the measured K_d and τ_c values were combined to form both average and median values for each month across the six sites. Gravimetric water content and bulk density were also reduced in a similar manner because these values were measured at the same time as K_d and τ_c .

The first step in the regression analysis was to calculate a correlation matrix using Pearson's correlation coefficient to determine which dependent variables were linearly correlated to the independent variables in the study, while also providing information about which independent variables were correlated. Scatter plots were also made to investigate any linear and nonlinear relationships between the independent and dependent variables. Any correlated independent variables were excluded from the same regression. The correlation matrix revealed three dependent variables with linear correlations to independent variables. These dependent variables were average bulk density, median bulk density, and average soil erodibility. Critical shear stress showed no linear correlation to any independent variable. Visual observation of scatter plots confirmed there were no linear or nonlinear relationships between τ_c and the explanatory variables. Independent variables correlated to the three dependent variables were then grouped into independent sets for the regression analysis. Ninety-two different groupings of independent variables were created.

The stepwise and regression tools within MINITAB were used to evaluate the independent variables. Stepwise regression was conducted on the 92 groupings of independent variables to identify possible relationships between K_d and τ_c and the independent weathering parameters. Regressions with all variables where coefficient p-values were greater than 0.05 were eliminated and regressions with both statistically significant and insignificant variables were rerun using the regular regression tool with only the statistically significant variables remaining in the regression. Regressions were examined further to remove any regressions that showed a lack of fit, as indicated by the Lack of Fit Test and the predicted R-square values (Minitab, 2003). Additionally, several regressions were very close replicates of other regressions. These regressions were compared using the PRESS statistic and only the best predictive relationships were considered. Any equations with significant single independent variables were also tested with the nonparametric Theil-Sen regression to ensure valid results (Sen, 1968; Theil, 1950). Theil-Sen regression is more robust with respect to outliers than regular least squares regression. All equations were then rerun with standardized data sets to

allow comparison of the coefficients of the independent variables to determine the relative influence of the independent variables. The data were standardized by subtracting the mean and dividing by the standard deviation.

Chapter 4 Results and Discussion

One jet test was performed at each of six experimental sites on Stroubles Creek each month for 12 consecutive months beginning in February of 2005 and concluding in January of 2006. During the course of this study, weather data were measured onsite, except for precipitation data during February 10 to March 23, 2005, during which time precipitation data from nearby rain gauges within the Stroubles Creek Watershed were used. This data loss was due to equipment malfunction. Historical climate data for the study region were obtained from the Southeast Regional Climate Center which operates within the Land, Water, and Conservation Division of the South Carolina Department of Natural Resources in Columbia, South Carolina (SERCC, 2005). Historic data averages developed from data spanning 1971 to 2000 from Blacksburg, VA, USA were used as the comparison for data gathered during this study. When compared to historical data, the air temperatures during the first half of the study, February through June, were below historical averages of maximum, minimum, and mean monthly temperatures. Temperatures during the second half of the study were consistently higher than historical averages for the mean minimum and maximum monthly temperature values (Figure 18). This comparison indicates that the study began under conditions of a colder winter than is typically experienced in the Blacksburg, VA area, while the winter months at the end of the study were milder than the historical record.

Rainfall levels were variable from month to month with the September 2005 monthly total of 9 mm being the least amount of rain measured during a one-month period (Figure 19). For the entire twelve month study, the rainfall total was 1060 mm. This annual total is only 25 mm below the historical yearly precipitation totals, making the study period fairly normal with respect to yearly total rainfall. Rainfall totals for June were normal while July and August had higher than normal rainfall totals. The higher rainfall totals during the summer could have reduced the occurrence of desiccation and wet/dry cycling. The winter season was generally wetter than average, with only February 2005 having lower than normal rainfall totals; therefore soil moisture likely did not limit ice formation within the bank soils.

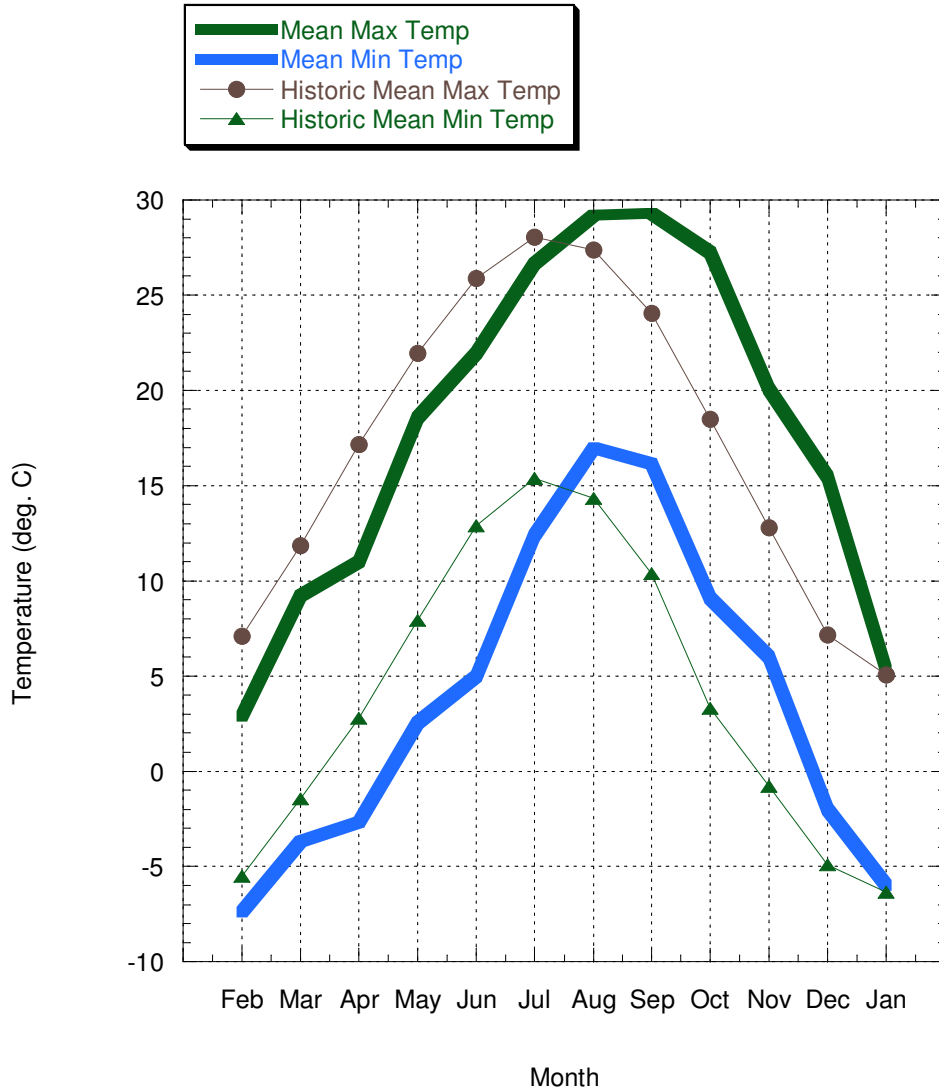


Figure 18 Monthly maximum and minimum actual and historical temperatures for the study time period for Blacksburg, VA, USA.

Descriptive statistics for K_d and τ_c are shown in Table 4.1. The mean τ_c and K_d values for the current study were 10.6 N/m^2 and $0.7 \text{ cm}^3/\text{N-s}$, respectively (Figure 22). Based on data from Hanson and Simon (2001) these streambanks soils varied from very erodible to resistant to erosion throughout the study. The most resistant streambank had a τ_c value of 43.3 N/m^2 during the month of November 2005, while the most erodible K_d value was recorded during the month of February at $8.6 \text{ cm}^3/\text{N-s}$. This measurement was not characteristic of the other measurements during February and was an order of magnitude greater than both the yearly mean of $0.7 \text{ cm}^3/\text{N-s}$ and the second highest K_d value of the month of $0.75 \text{ cm}^3/\text{N-s}$. The least resistant streambank

had a τ_c value of 0 N/m² while the least erodible streambank had a K_d value of 0.01 cm³/N-s. In a similar study in southwestern Virginia, Wynn and Mostaghimi (2006b) measured mean τ_c and K_d values of 3.5 N/m² and 2.87 cm³/N-s, with ranges of 0 - 21.9 N/m² and 0.2 - 13.1 cm³/N-s, respectively.

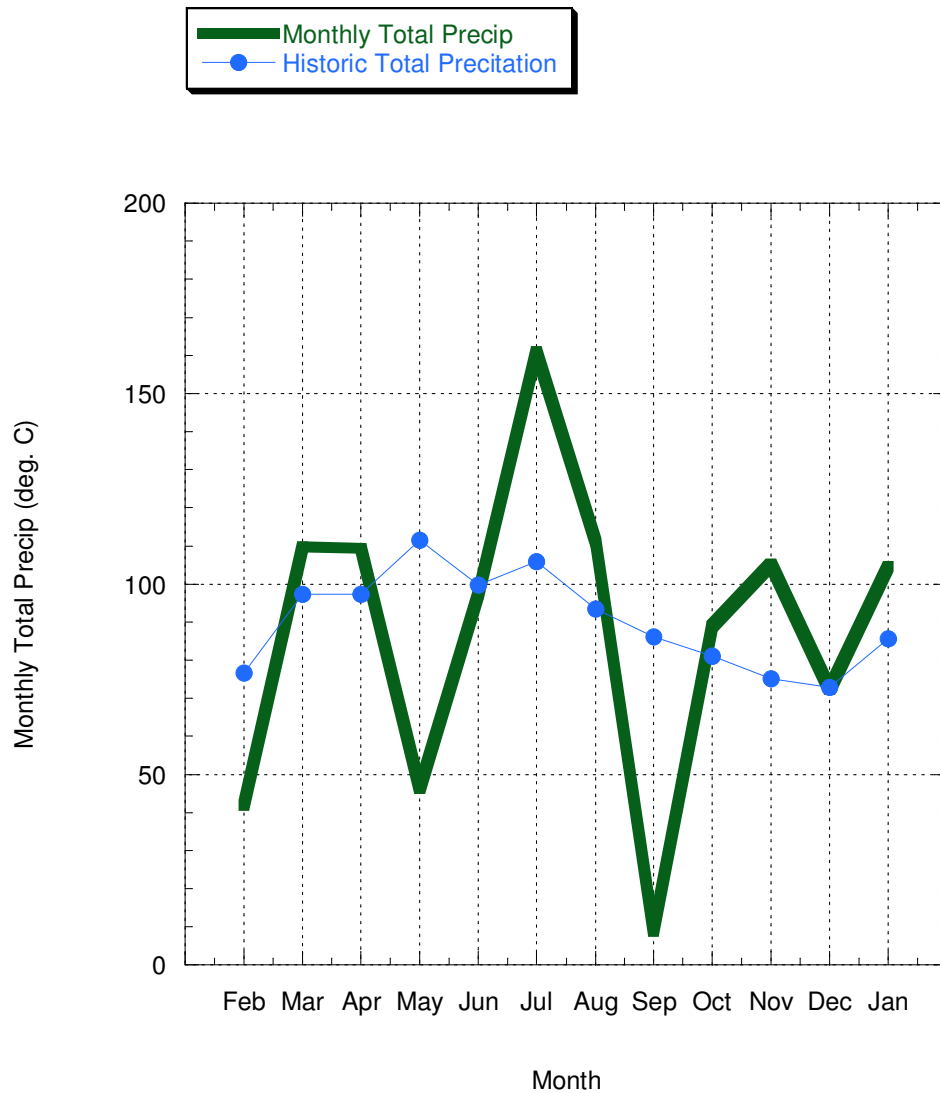


Figure 19 Actual monthly precipitation totals during the study period and historical monthly precipitation totals from Blacksburg, VA, USA.

Both τ_c and K_d have been reported to vary widely even within a given stream reach. Wynn and Mostaghimi (2006b) found that at one site, τ_c and K_d varied by four and one orders of magnitude, respectively. In the current study, a similar relationship was found within monthly τ_c

and K_d values. During the months of January and July, τ_c varied by four orders of magnitude and K_d varied by one order. Hanson and Simon (2001) found a range of τ_c and K_d values of six and four orders of magnitude, respectively, for measurements of Loess soils in several regions of the midwestern USA. Hanson and Simon (2001) attributed these variations to subaerial exposure, weathering processes, and cracking along planes of weakness. These first two sources of error were likely not responsible for the spatial variability in this study. Because data differing by several orders of magnitude were taken at the same location at approximately the same time, it was assumed these reaches were exposed to the same subaerial conditions and weathering processes. The more realistic explanation for the range of values in the current study is that localized variations in bank material or bank conditions caused the differences in τ_c and K_d values. Examples of these localized conditions often observed during data collection are gravel lenses, crayfish burrows, muskrat tunnels, plant material growing from the bank, and bank instability due to the initial phases of mass failure.

In an unpublished study designed to evaluate the precision of the jet test, uniform, remolded blocks of silt loam soil were tested (Summers et al., 2006). These blocks had a range of τ_c values from 0.45 to 1.5 N/m² and K_d values from 1.3 to 3.0 cm³/N-s. The standard deviation of τ_c was 0.4 N/m² while the standard deviation for K_d was 0.5 cm³/N-s. A box plot of the data collected for this study is shown in Figure 20. When compared to the year of sampled data from Stroubles Creek, VA, the data measured for uniform soil samples with a consistent bulk density and soil moisture had less variability than the field study on naturally occurring soils. Standard deviations from the field study on naturally occurring soils differed from the remolded block study by one order of magnitude for K_d and two orders of magnitude for τ_c . This finding indicates there are processes independent of the jet test procedure that cause large variability in τ_c and K_d . Both spatial and temporal variability in natural soils are possible explanations for the larger standard deviations in the field studies.

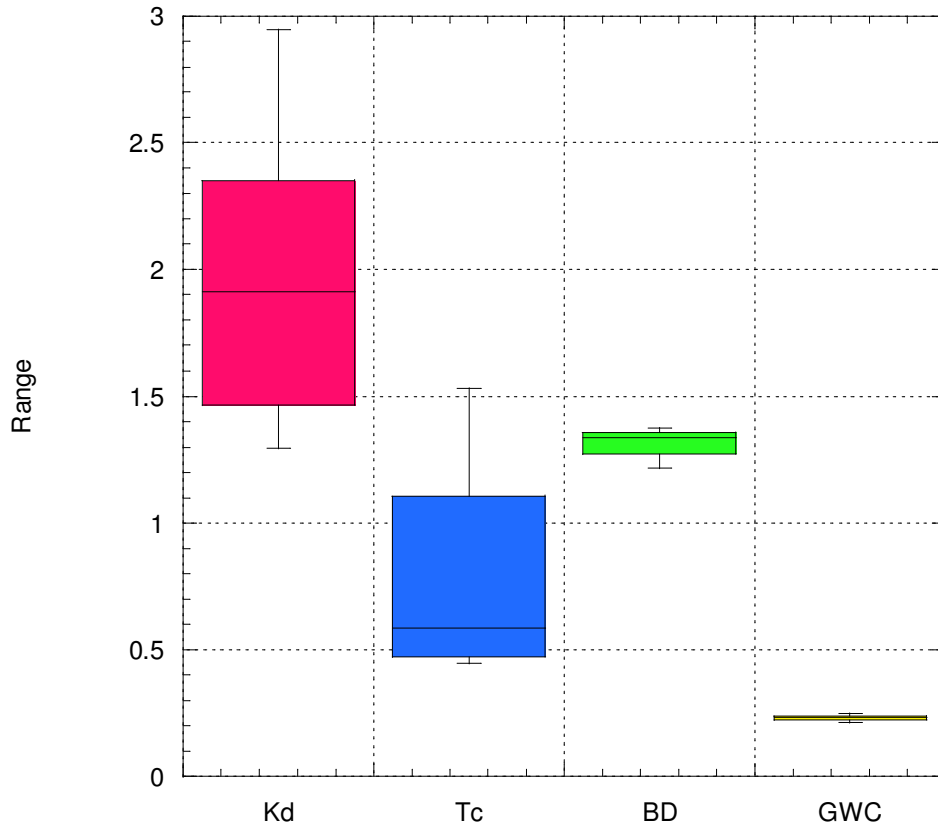


Figure 20 Unpublished data from jet test evaluation study using remolded soil blocks of silt loam soil. K_d represents soil erodibility ($\text{cm}^3/\text{N}\cdot\text{s}$), τ_c represents critical shear stress (N/m^2), BD represents bulk density (g/cm^3), and GWC represents gravimetric water content (g/g).

The paired K_d and τ_c values from the current study and Wynn and Mostaghimi (2006b) were consistent with trends observed by both Hanson and Simon (2001) and Arulanandan et al. (1980) where higher τ_c values corresponded with lower values of K_d and vice versa (Hanson and Simon, 2001). A similar trend was found during this study and is presented in Figure 21, with erodibility categories developed by Hanson and Simon (2001). Hanson and Simon (2001) tested three different stream networks in the loess area of the Midwestern USA and showed a large degree of variation within the individual stream networks and across the three separate areas. Data from this study fell mainly in the erodible and moderately resistant categories while Hanson and Simon (2001) and Wynn (2004) had greater distributions throughout all the categories. This difference is explained by the fact that one location was studied during this research while multiple locations were studied by both Hanson and Simon (2001) and Wynn (2004). These

results show that even along the same stream reach, both K_d and τ_c vary over several orders of magnitude. This variability can be attributed to changes in subaerial processes.

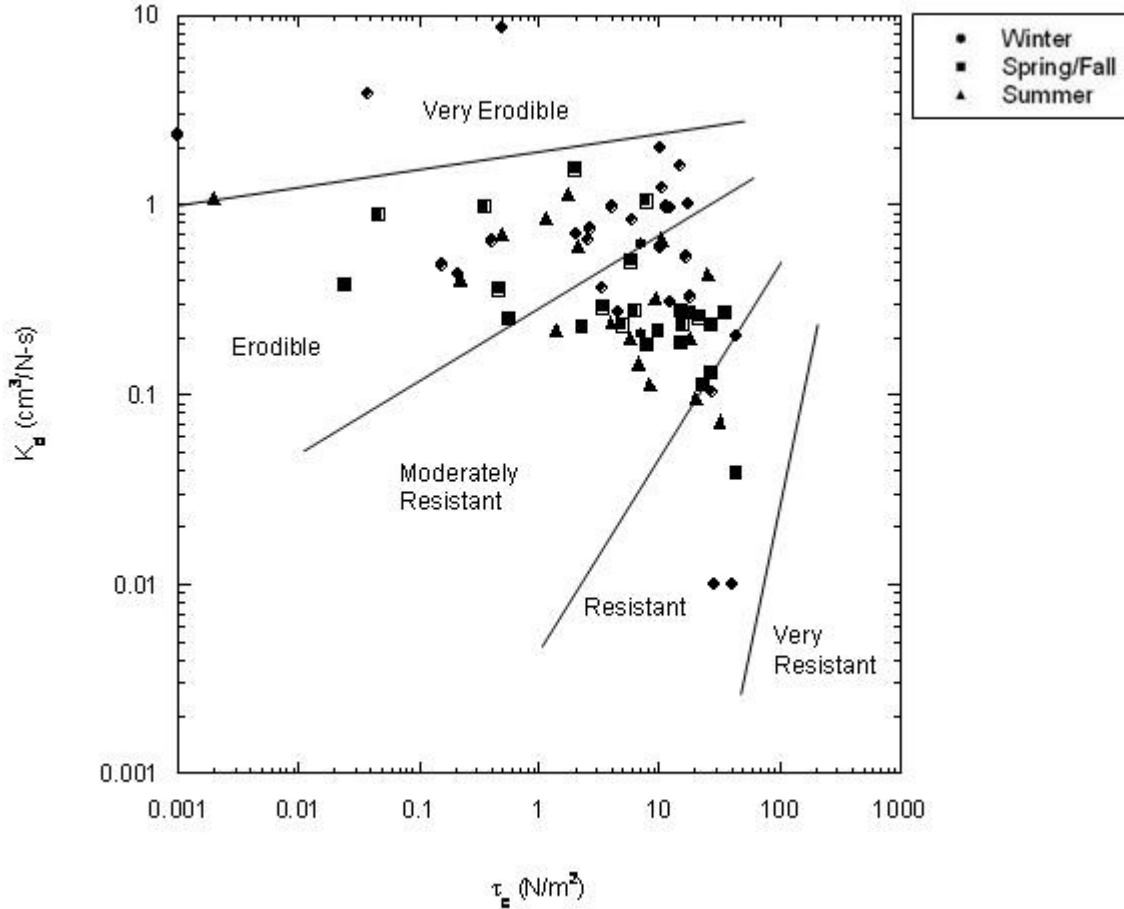


Figure 21 Plot of soil erodibility versus critical shear stress from data collected between February 2005 and January 2006 on Stroubles Creek, VA, USA.

Another difference between the results of this study and that of Hanson and Simon (2001) and Wynn (2004) is illustrated in Figure 22. For this study, K_d generally remained below $2 \text{ cm}^3/\text{N-s}$, while τ_c varied over an order of magnitude. This distribution is in contrast to the two previously mentioned studies by Hanson and Simon (2001) and Wynn (2004) where there was a strong, inverse relationship between K_d and τ_c . Figure 22 shows that K_d remained fairly constant throughout the study, while τ_c varied tremendously. Several researchers have questioned the validity of a critical shear stress. Turbulent stream flows make defining the point of incipient motion difficult (Chang, 2002; Lavelle, 1987), which leads to many researchers either consider

τ_c insignificant or zero (Foster et al., 1977; Hanson, 1990, 1999; Temple and Alspach, 1992) or assign a constant value based on soil properties (Temple, 1980, 1983, 1985).

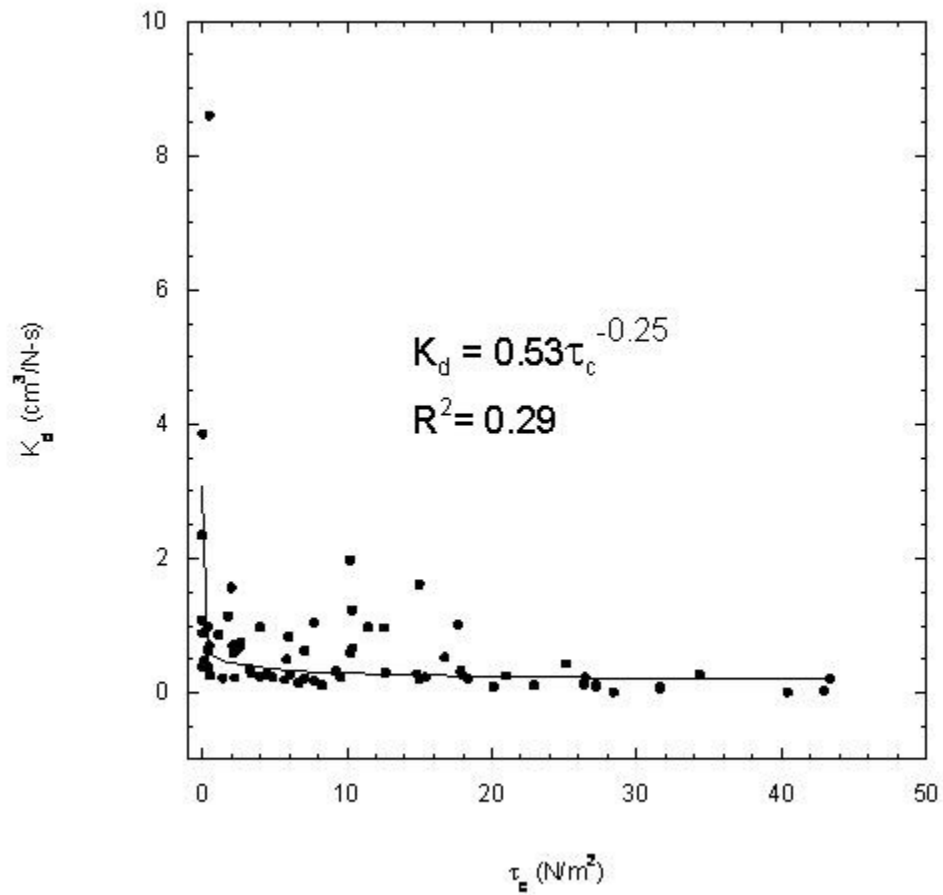


Figure 22 Soil erodibility and critical shear stress scatter plot with power curve trend line for Stroubles Creek near Blacksburg, Virginia, USA.

Table 4.1 Descriptive statistics for soil erodibility and critical shear stress data sets during the study period on Stroubles Creek, VA, USA.

Variable	N	Mean	Median	Minimum	Maximum	Range	Standard Deviation	Variance	Coefficient of Variance	1st Quartile	3rd Quartile	IQR[%]
τ_c^*	71	10.6	7.1	0	43.3	43.3	11.1	124.2	105.7	1.8	16.7	14.9
K_d^+	71	0.7	0.4	0.01	8.6	8.6	1.1	1.3	159.4	0.2	0.9	0.6

* = critical shear stress (N/m²)

+ = soil erodibility (cm³/N-s)

% = inner quartile range

Both K_d and τ_c varied dramatically from month to month, while average values of bulk density (BD) remained relatively constant, despite the presence of outliers. Box plots of the mean monthly K_d and τ_c are shown in Figure 26 and Figure 27, respectively. While there were no obvious seasonal trends in τ_c values, the K_d data were highest during the winter and summer, when subaerial processes were likely most active. There were few outliers in the τ_c measurements, but the range of monthly values was greater. The highest monthly average K_d values occurred during the months of February and March while the lowest monthly average τ_c values occurred during January and August. This increased susceptibility was likely due to increased moisture and freeze-thaw cycling during the winter months of January, February, and March, and an increase in desiccation cracking in August due to high temperatures and solar radiation.

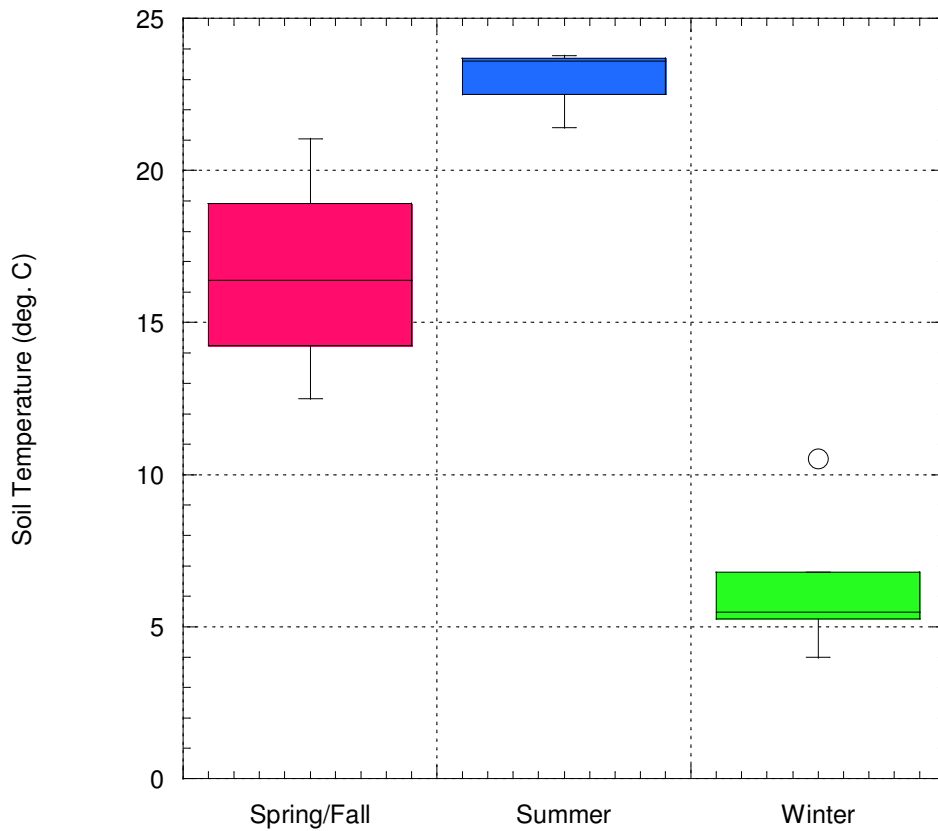


Figure 23 Seasonal average monthly soil temperature for the period February 2005 through January 2006 along Stroubles Creek near Blacksburg, Virginia, USA.

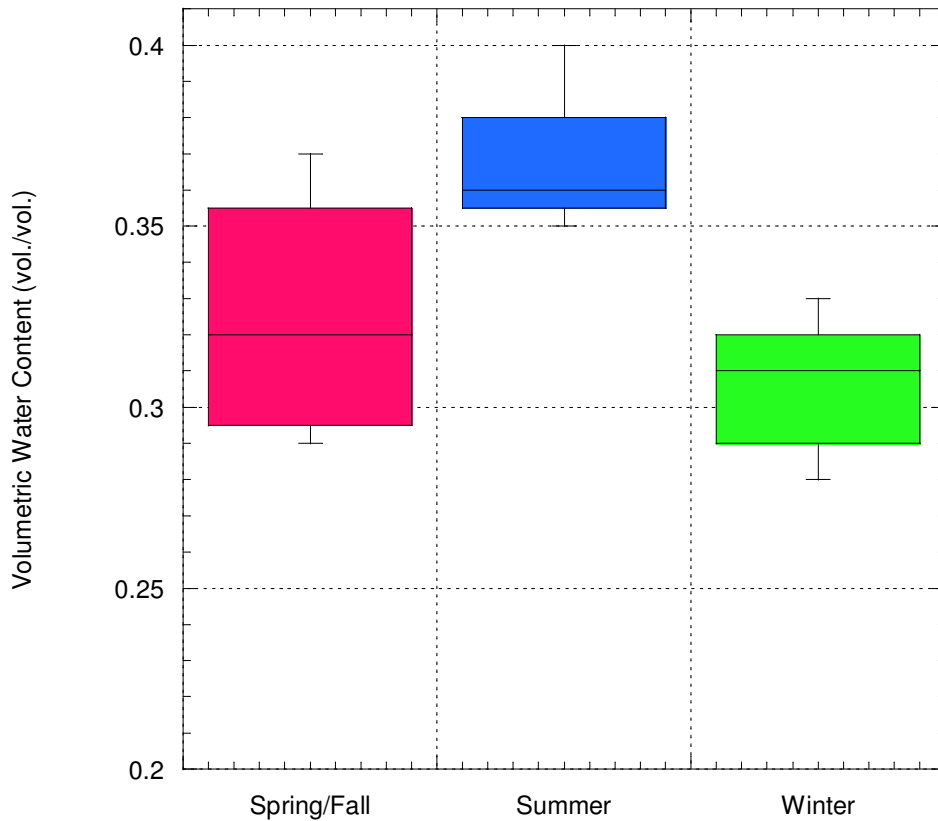


Figure 24 Seasonal average monthly soil volumetric moisture content for the period February 2005 through January 2006 along Stroubles Creek near Blacksburg, Virginia, USA.

In contrast, the streambank was least susceptible to erosion during the months of May and October according to K_d values and October and November according to τ_c values. The lack of weathering conditions during the months of May, October, and November caused by moderate temperatures with no extreme wet-dry or freeze-thaw conditions lead to high τ_c values and low K_d values. Soil bulk density was also measured monthly because it is an easy to measure property that is strongly correlated to soil erodibility (Wynn and Mostaghimi, 2006b). The bulk density (BD) data are plotted in Figure 28. While some months, such as March 2005 had a large range in BD, the average value remained relatively constant in the range of 1.2-1.4 g/cm³.

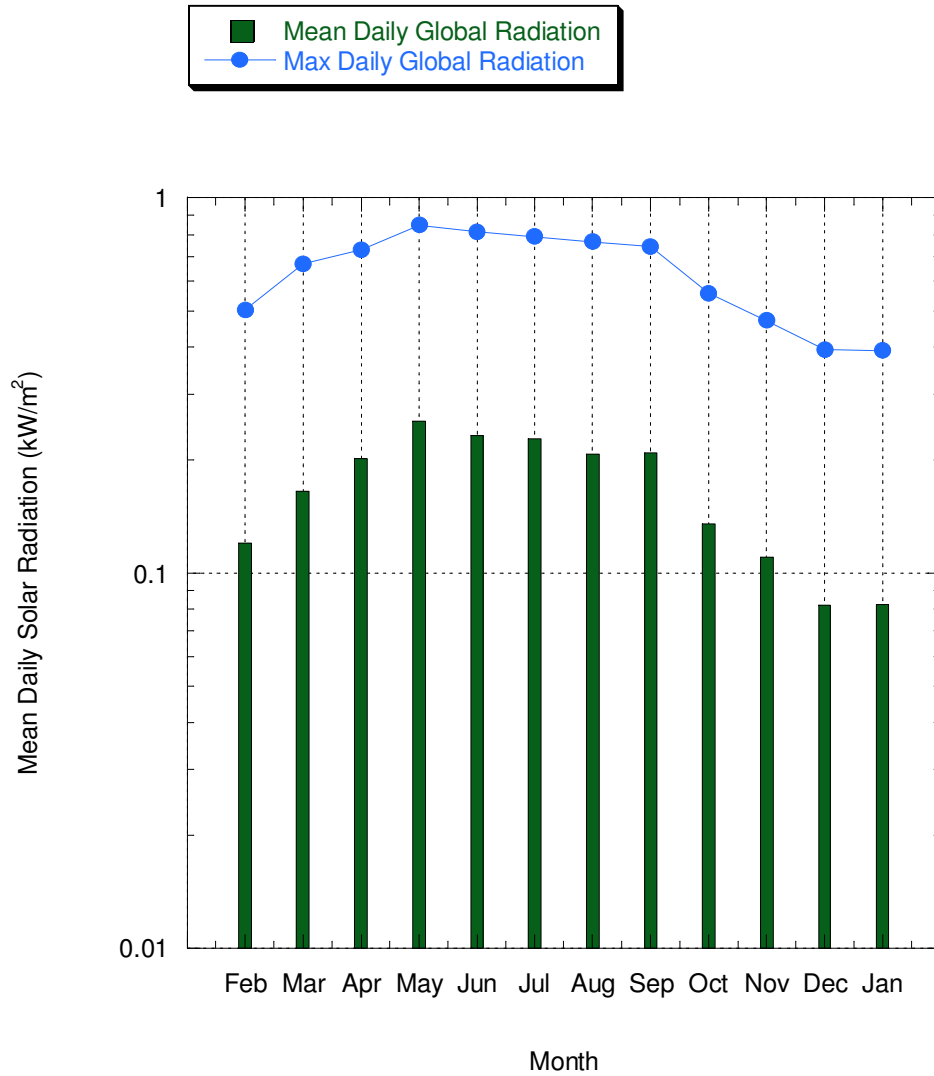


Figure 25 Mean and maximum solar radiation values for February 2005 through January 2006 from Kentland Farm, Blacksburg, VA, USA.

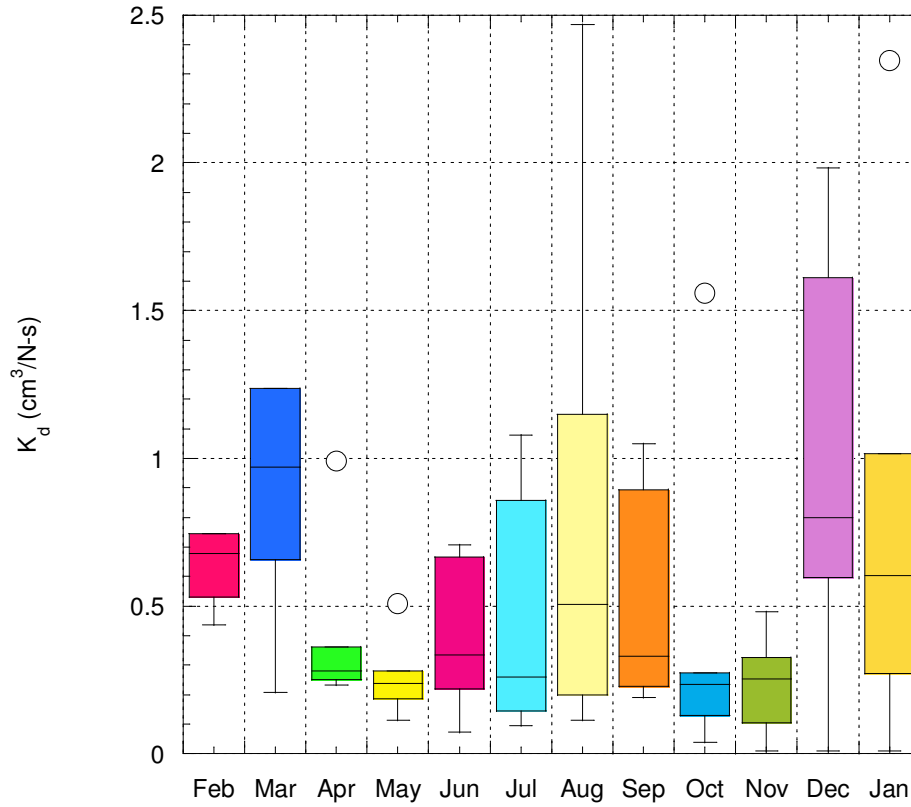


Figure 26 Box plot of soil erodibility (K_d) by month along Stroubles Creek near Blacksburg, Virginia, USA. February and March outliers are 8.6 and 3.9 $\text{cm}^3/\text{N}\cdot\text{s}$, respectively, but do not appear due to rescaling of Y-axis.

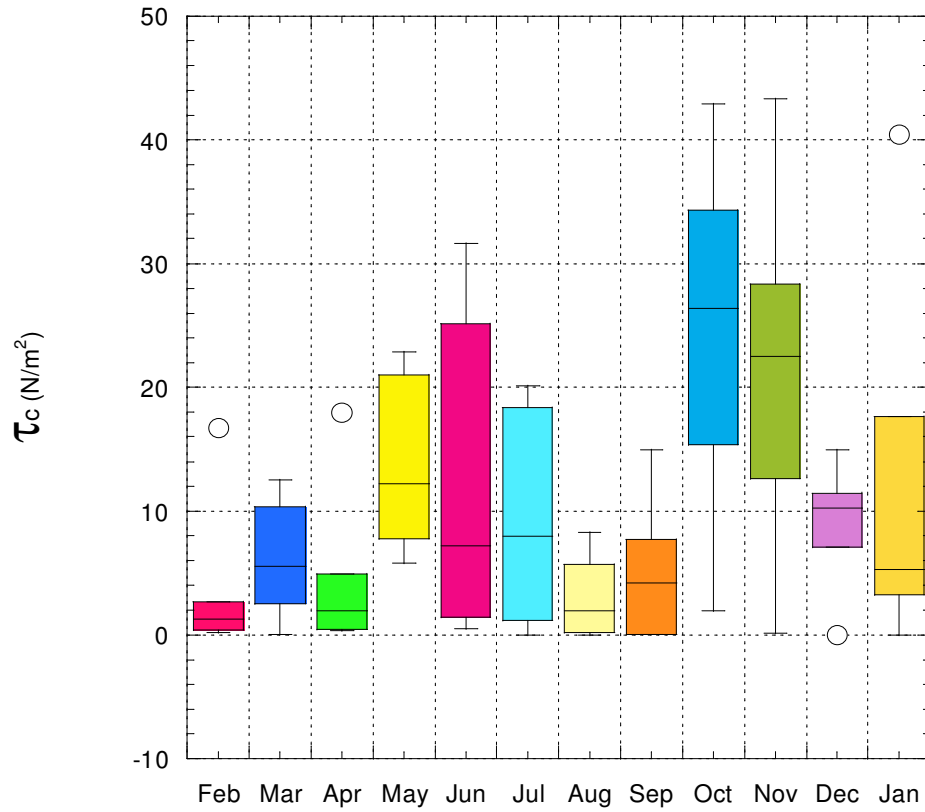


Figure 27 Box plot of critical shear stress (τ_c) by month along Stroubles Creek near Blacksburg, Virginia, USA.

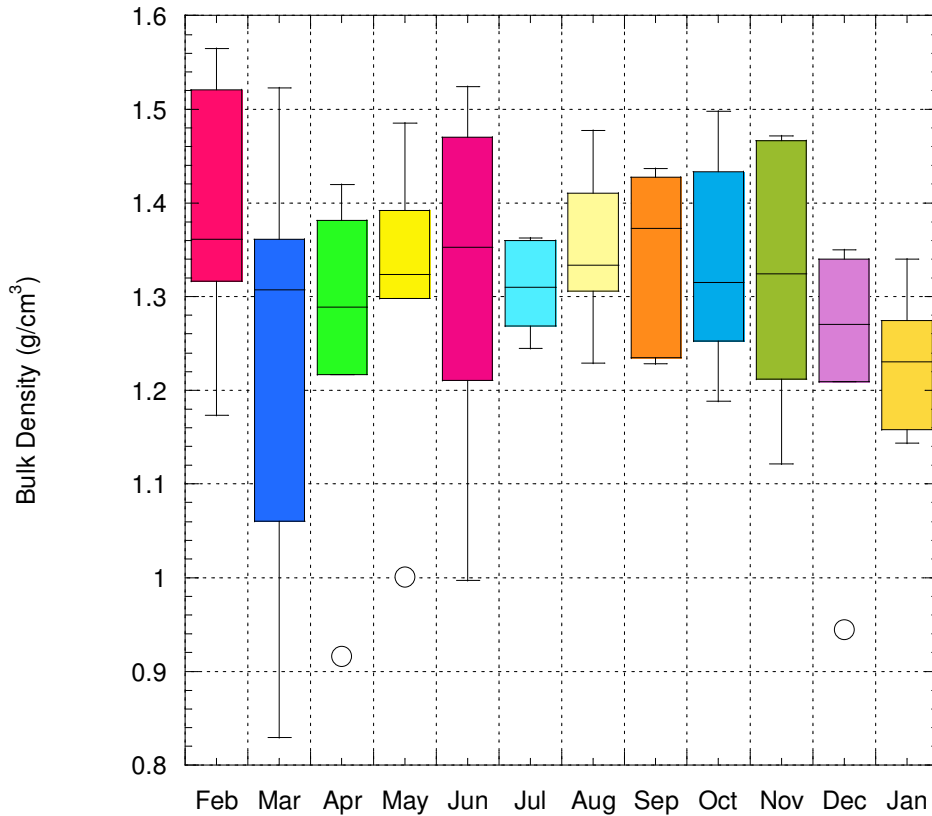


Figure 28 Box plot of bulk density (BD) by month along Stroubles Creek near Blacksburg, Virginia, USA.

4.1 Seasonal Variability of K_d and τ_c

Seasonal differences in K_d , τ_c , and BD are shown in Figure 30, Figure 31, Figure 32, respectively. The median winter K_d was 75 percent higher than the median summer values and 1.4 times higher than the mean Spring/Fall values. The median Spring/Fall τ_c was 38 percent greater than the mean Summer values and only 8 percent higher than median winter values. Bulk density changed less than 4 percent from season to season. Statistical differences among the seasons were evaluated using a nonparametric alternative to ANOVA and a nonparametric multiple comparison test (Helsel and Hirsch, 1993; Zar, 1999). The Kruskal-Wallis test was run with a data set of 71 entries due to problems with the jet test on Site 1 during December 2005. The Kruskal-Wallis test showed significant differences between soil erodibility seasonal group

medians, while no statistically significant differences were determined between the seasonal groups for critical shear stress or bulk density at $\alpha=0.05$. A possible explanation for a lack of significance with regards to critical shear stress is that critical shear stress displayed a much greater variability than soil erodibility. This variability overshadowed any possible seasonal trends and made development of statistically significant relationships unsuccessful.

Results of Dunn's test showed soil erodibility during Winter months, as grouped by the cluster analysis, was statistically different from soil erodibility during the Spring/Fall months. This means that the soil erodibility during the Winter was greater than that of the Spring/Fall grouping. No evidence was found to suggest that Winter and Summer soil erodibility were different or that Summer soil erodibility was statistically different from Spring/Fall soil erodibility. The lack of significant difference between the Summer erodibility and Winter or Spring/Fall erodibility could have resulted from the unusually high rainfall during the summer of 2005. This rainfall increased soil moisture, minimizing soil desiccation. Average monthly soil volumetric moisture content values are shown in Figure 29. These findings demonstrates quantifiably that soil erodibility is greater in the Winter, lending credence to the observations of Wolman (1959), Twidale (1964), Hooke (1979), Knighton (1973), and Thorne and Lewin (1979).

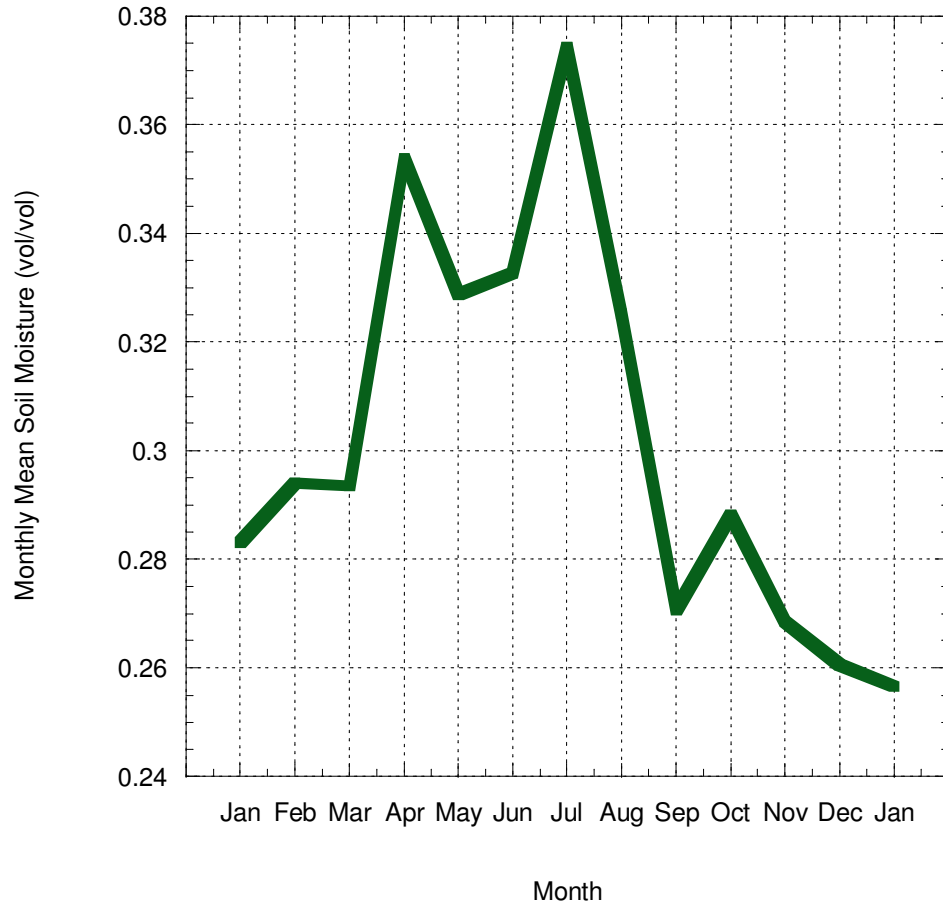


Figure 29 Monthly mean soil moisture content for banks along Stroubles Creek, near Blacksburg, Virginia, USA.

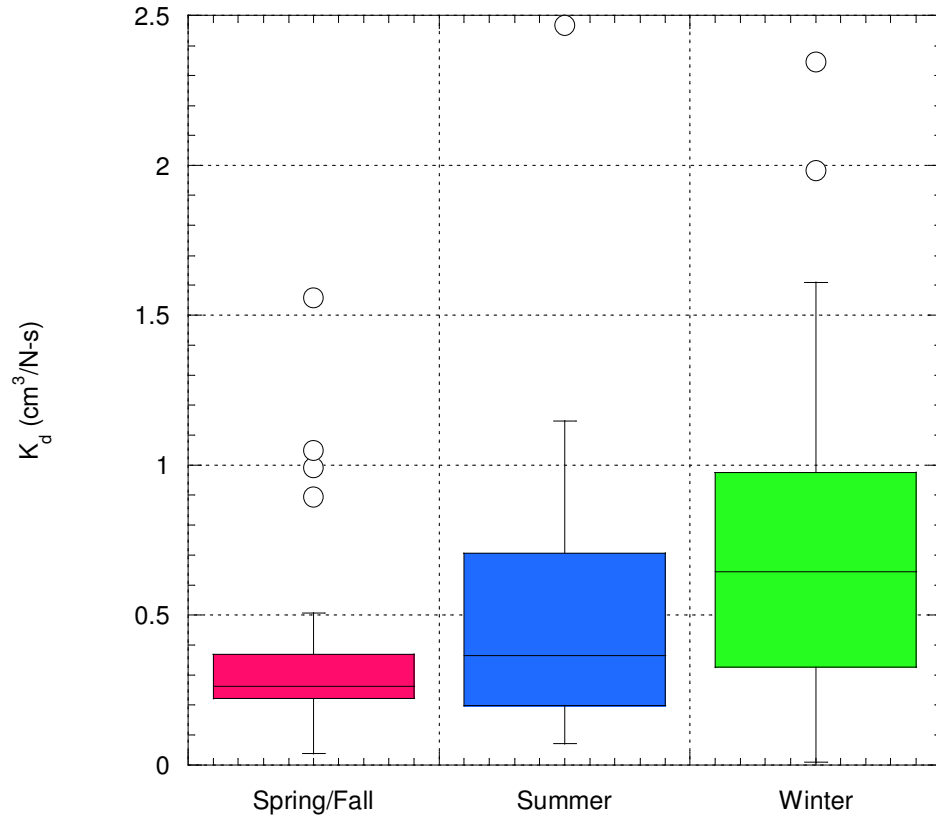


Figure 30 Seasonal K_d values along Stroubles Creek near Blacksburg, Virginia, USA, with two winter outliers of 8.6 and 3.9 $\text{cm}^3/\text{N-s}$ were eliminated from the figure.

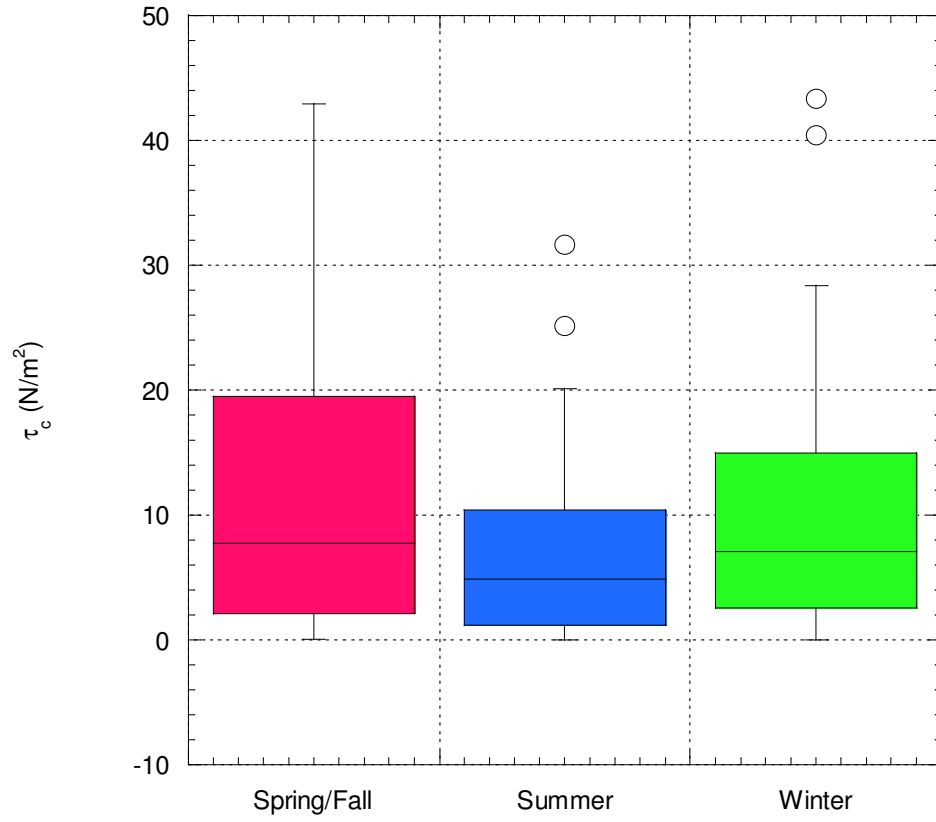


Figure 31 Seasonal τ_c values along Stroubles Creek near Blacksburg, Virginia, USA.

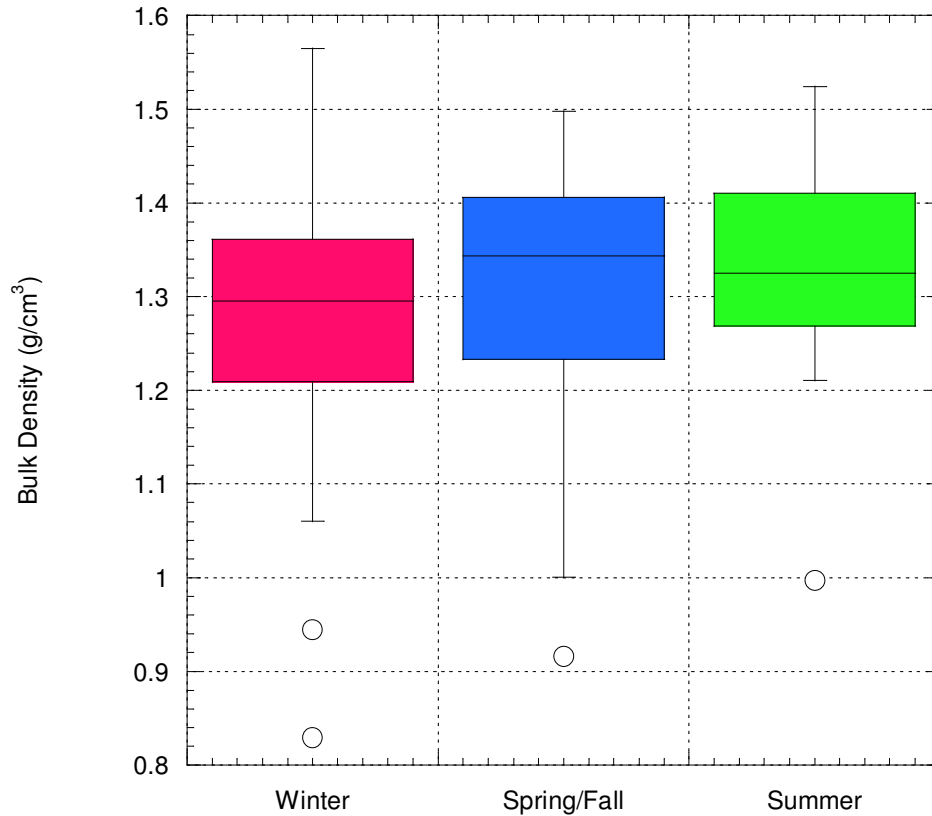


Figure 32 Seasonal bulk density values along Stroubles Creek near Blacksburg, Virginia, USA,

The results of the multiple comparison test indicated there was evidence that soil erodibility changes as environmental conditions influencing soil weathering change. The box plot in Figure 30 shows that the Winter soil erodibility (K_d) has a much larger variability than either the Summer or the Spring/Fall seasons. The Winter K_d values include both the minimum and maximum values for the entire study of 0.01 and 8.6 $\text{cm}^3/\text{N-s}$, respectively. The Spring/Fall season shows the smallest difference between the lower and upper quartiles, which indicates more consistency and stability with the soil conditions than in the Winter or Summer.

A Kruskal-Wallis test was also performed on the τ_c , K_d , bulk density, and GWC data to examine if there were any statistically significant differences between the six different data collection areas. The Kruskal-Wallis test showed that no statistically significant differences existed between the soils at the sites, thus, monthly variances in soil data from site to site were not due to systematic differences in soil parameters at individual sites. The Kruskal-Wallis test

did find that the gravimetric water content of all the sites were not identical. At least one site is different from the group as indicated by the p-value of 0.006. The Dunn multiple comparison test showed that only Sites 5 and 6 had a statistically significant difference between them. Site 5 and Site 6 are seen in Figure 33 as having the greatest difference in medians. The other sites have medians close enough to not be statistically significant.

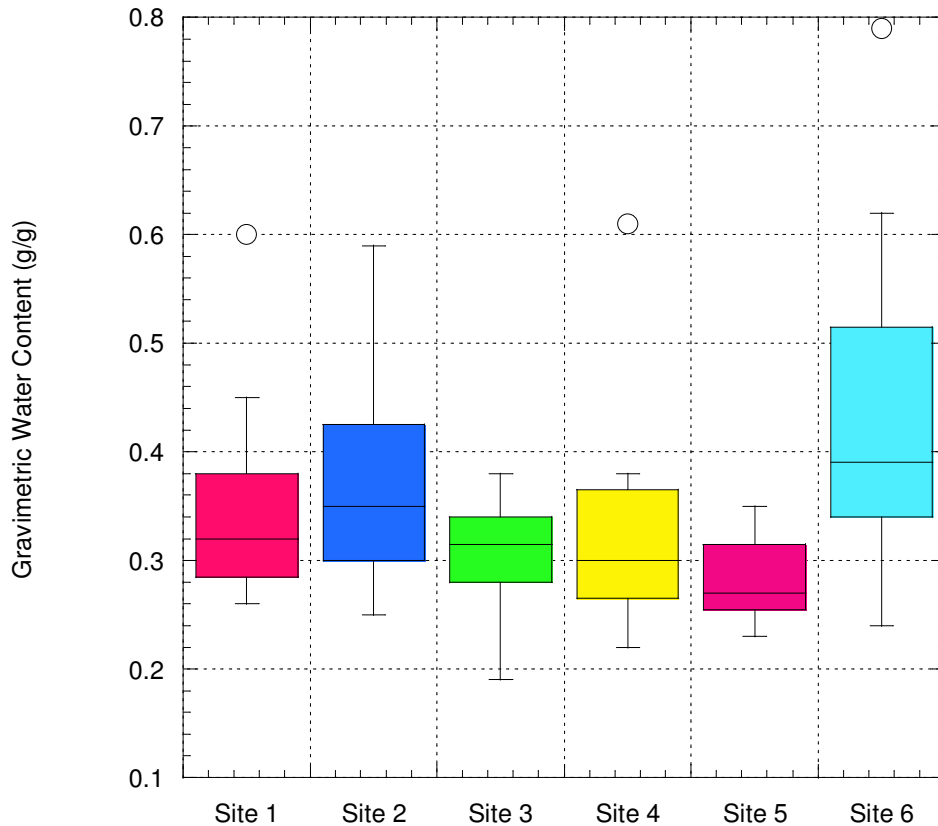


Figure 33 Gravimetric Water Content by site along Stroubles Creek near Blacksburg, Virginia, USA.

General field observations also confirm the results presented in Figure 34. While conducting jet tests, streambanks were observed to have very moist, loose outer layers of soil during the winter months. These soil layers were easily removed by the initial five minutes of jet testing or by simply brushing the surface with hand or tool. Behind the surface layer of soil was a denser, undisturbed soil layer which was soft to the touch due to an increase in moisture during the winter months but was not as delicate as the surface soils. In contrast to these observations,

the streambank of Stroubles Creek during the summer months was often hard, compact, and covered with desiccation cracks. Summer sunshine and heat often led to loose, dry sand on the streambank surface that was easily brushed away. This layer was also readily removed by jet testing. Beneath both the desiccation cracks and the dry, loose, sandy soil layer was a generally firm, solid soil layer with sufficient structure to withstand physical contact. While jet testing, if the streambank section being tested did not possess a surface layer of loose or easily erodible material, the scour hole from the jet test device was very shallow, indicating a resistant soil.

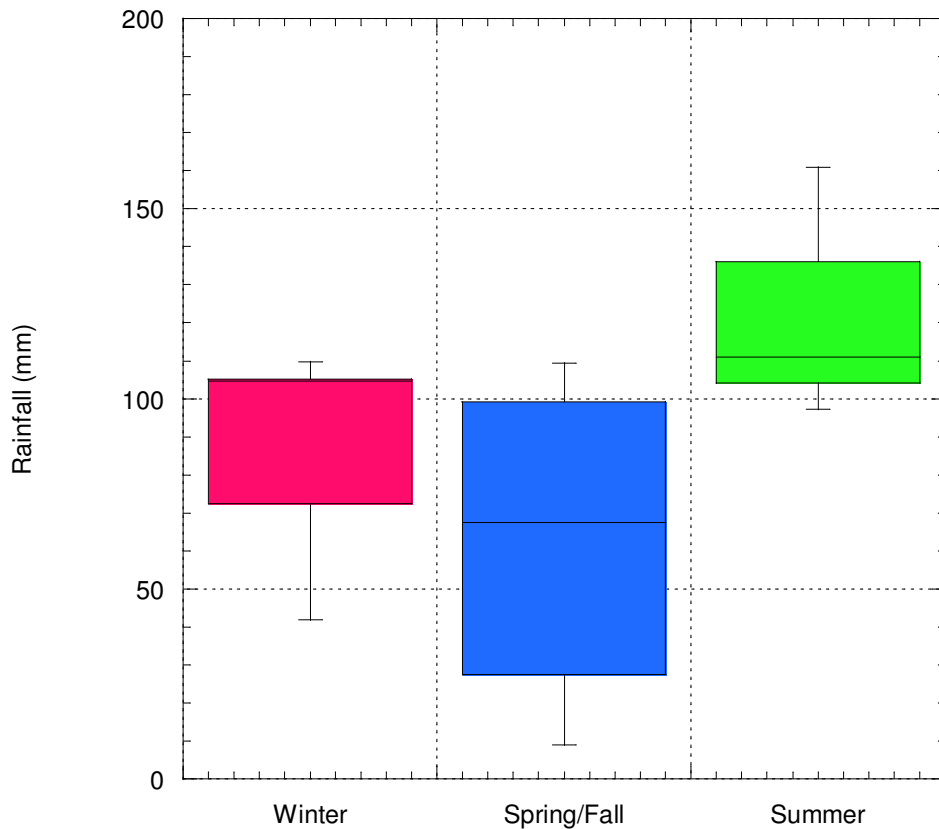


Figure 34 Seasonal monthly rainfall totals for the period February 2005 through January 2006 near Blacksburg, Virginia, USA.

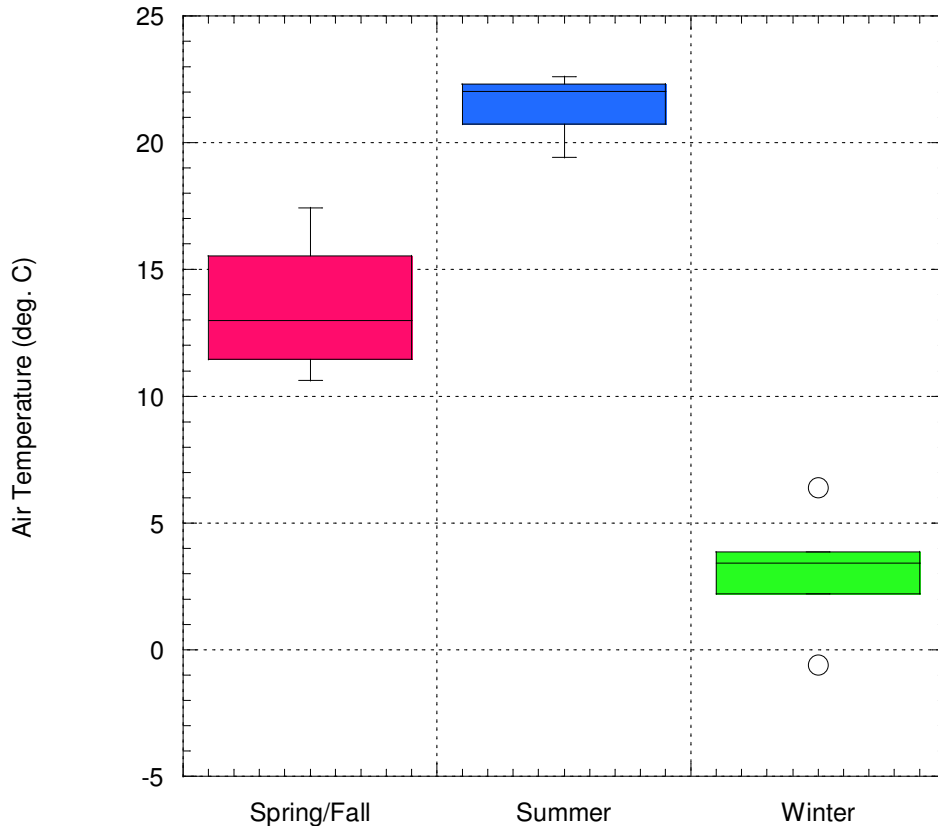


Figure 35 Seasonal average monthly air temperature for the period February 2005 through January 2006 near Blacksburg, Virginia, USA.

4.2 Weathering Influences on K_d and τ_c

Multiple linear regression analysis was conducted using the dependent variables bulk density, critical shear stress, and soil erodibility. Independent variables for the regressions were developed primarily from air temperature, soil temperature, soil moisture, number of freeze-thaw cycles, and stream stage data. Freeze-thaw cycles occurred between the months of November and April with the majority of freezing occurring within the months of January 2005, February, March, and December 2005, and January 2006 (Figure 36).

Mineralogical analyses revealed the clay mineralogy of the streambank soils may have influenced the effects of surface weathering. High percentages of montmorillonite are present along the banks of Stroubles Creek. Approximately 25 percent of the makeup of the soil is montmorillonite (Table 4.2). Montmorillonite is known to be very prone to shrink-swell

behavior. The expansion of the montmorillonite layers is due to the weak charge present within the layer silicates. This structure makes montmorillonite susceptible to water infiltrating and separating the layer silicates. Once the layer silicates are separated, the electrochemical bonds become even weaker due to Coulombs Law; which states the forces of attraction between charges diminishes exponentially as the distance between the charges increases. With respect to erosion, this reduced attraction allows for easier removal of soil particles because less shear stress is needed to overcome the interparticle forces maintaining the layer bonds. The remaining minerals found within the streambank soil from Stroubles Creek do are all resistant to layer expansion.

Table 4.2 Mineralogical analyses results for composite bank material taken from along Stroubles Creek near Blacksburg, VA, USA.

Stroubles Creek Bank Material	% Layer Silicate
Kaolinite	35%
Montmorillonite	25%
Mica/Illite	20%
Hydroxy-interlayered Vermiculite	15%
Chlorite	3%
Quartz	2%

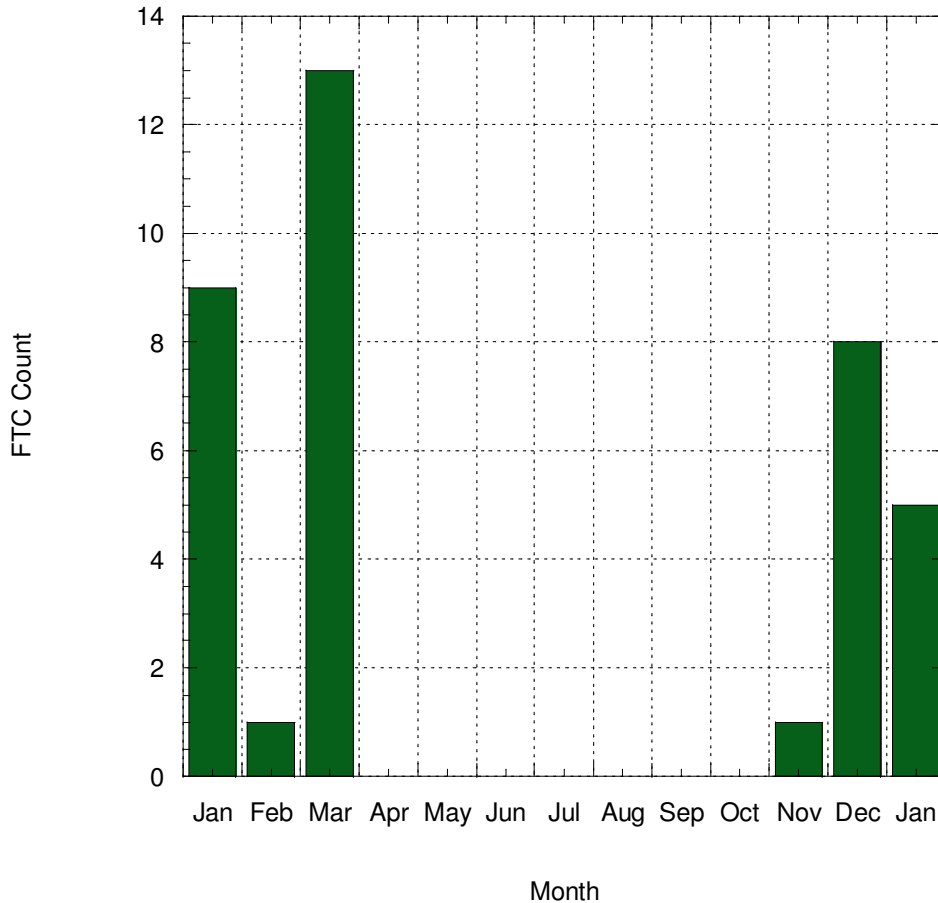


Figure 36 Freeze-thaw cycle count by month along Stroubles Creek near Blacksburg, Virginia, USA. Freeze-thaw cycles were determined by counting transitions from below 1°C to above 1°C.

Regression equations were developed by comparing the dependent soil variables found through monthly jet testing and soil sampling to continuously-monitored environmental data. A correlation matrix was calculated using 94 sets of monthly variables. From these 94 sets of data, 92 equations were developed utilizing only independent variables strongly correlated to the dependent variables yet not correlated to any other independent variables within the same regression equation. The 92 equations consisted of two and three independent variables which were then examined using the regression function within MINITAB. From the 92 original equations developed, 30 equations were statistically significant at $\alpha=0.5$. Regression equations with either a p-values greater than 0.05 or a significant lack of fit test (p-value less than 0.1) were eliminated. Several regression equations with similar independent variables with large residuals, large influence, a lower adjusted r^2 value, or a high PRESS statistic were also eliminated. An

example of similar independent variables was gravimetric (g/g) and volumetric (vol/vol) water content measurement derived from the monthly soil samples. Both variables indicated the amount of moisture in the soil but expressed it with different units. A summary of the resulting regression equations are shown in Table 4.3. Included in the table are the results of the nonparametric Theil-Sen regression that was performed to confirm the results of the single linear regressions (Hollander and Wolfe, 1973; Sen, 1968; Theil, 1950). These regressions had either large residuals or large influence but they all proved statistically significant as a result of the Theil-Sen regression. Of the three dependent variables analyzed, bulk density was more strongly correlated to the environmental data than either soil erodibility or critical shear stress. Both median monthly bulk density (M_BD) and average monthly bulk density (A_BD) showed strong correlation to gravimetric moisture content and the number of freeze-thaw cycles. This strong correlation was likely because bulk density is a composite soil property that captures features such as soil texture, clay content, and porosity (Wolman, 1959). Additionally, bulk density is a relatively simple measurement with low variability; as noted previously, both K_d and τ_c vary over several orders of magnitude, even at a single site.

The number of freeze-thaw cycles during the 30 days prior to jet testing (as represented by “FTC_30D_{M<0.5}” in Table 4.3) explained a high degree of variance (70%; $p=0.000$) in K_d (as represented by “Kd” in Table 4.3). The Theil-Sen regression performed for these variables also yielded a significant regression with a p-value of 0.0197, which confirms the findings of the parametric tests. As the number of freeze-thaw cycles increased in the 30 days prior to jet testing, the streambank soil erodibility increased. Doubling the number of freeze-thaw cycles per month increased K_d by 200 percent. This finding has significant repercussions because it directly links an increase in soil erodibility to a major winter weathering process, providing quantitative support of previous observations by Wolman (1959), Twidale (1964), Hooke (1979), Thorne and Lewin (1979). With such a high adjusted R^2 value, the number of freeze-thaw cycles in the 30 days preceding a flooding event is a significant influence over erosion processes. In a study on the effects of riparian vegetation on soil erosion, Wynn and Mostaghimi (2006b) found that soil erodibility increased with the number of freeze-thaw cycles for certain soils. The authors also found bulk density was a significant factor in determining streambank erodibility. While this study failed to establish a link between bulk density and soil erodibility, the fact that bulk density was significant predictor of erodibility for Wynn and Mostaghimi (2006b) supports

the findings of this study that soil moisture and freeze-thaw cycling significantly influence both soil erodibility and bulk density.

Even though only one significant regression equation was developed utilizing soil erodibility and no significant regression equations for critical shear stress were developed, previous studies concluded bulk density is a very important with regards to streambank erosion processes. As with the seasonal variations in critical shear stress, the regression analyses were unable to identify statistically significant relationships between subaerial processes and critical shear stress. Critical shear stress results appeared more sensitive to variations in the soil surface than soil erodibility. In a study using the same jet test equipment to study streambanks in the southwest Virginia area, Wynn and Mostaghimi (2006b) found the most influential factor on soil erosion rates was bulk density; K_d was inversely related to bulk density. Hanson and Robinson (1993) also found that soil dry weight following compaction influenced soil erodibility and stated compaction and erodibility are “interdependent” inversely correlated soil properties. Wynn and Mostaghimi (2006b) believed bulk density was an important explanatory variable for critical shear stress and soil erodibility because it encompassed multiple soil properties (soil texture, soil chemistry, root density, and soil organic matter content) in one variable. Additionally, due to the ease of measurement, bulk density has less measurement error than K_d or τ_c . Wynn and Mostaghimi (2006b) found bulk density explained as much as 52 percent of variance in soil erodibility and 46 percent of variance in critical shear stress.

In this study, soil moisture and freeze-thaw cycling explained more than 80 percent of the variance in bulk density. Significant correlation between bulk density and gravimetric water content and freeze-thaw cycles was developed (adjusted $R^2 = 0.855$). This strong relationship can be attributed to the fact that the bulk density sample was taken from as close to the streambank surface as possible, which allowed soil moisture and freeze-thaw processes to have a greater impact on the soil characteristics than if the sample had been taken from deeper into the bank. Because these regression equations were developed using standardized values, the results can be used to compare influences on the dependent variables made by the different independent variables. The coefficients from one bulk density regression equation were 0.65 for soil moisture and 0.43 for freeze-thaw cycling, indicating bulk density was influenced more by soil moisture content than by freeze-thaw cycling. Wynn and Mostaghimi (2006b) sampled bulk density with a larger bulk density ring (5-cm x 5-cm) than the rings used in this study (5-cm x 2.5-cm) which

could explain why this study produced such a high R^2 . This finding provides quantitative evidence for the widely held belief that both soil moisture and freeze-thaw cycling are the main processes of subaerial erosion.

Soil moisture changes are responsible for wetting and drying, which previous studies found to impact streambank erosion (Lawler et al., 1997a). Increases in moisture content combined with a decrease in freeze-thaw cycles were shown to increase bulk density. An explanation for this occurrence was found when the rainfall and soil moisture data were evaluated Figure 33 and Figure 34. In this study, greater precipitation and higher soil moisture content were measured during the summer months than the winter months, despite the fact that winter is typically the season with higher soil moisture contents due to less evapotranspiration and lower air temperatures. The bulk density regression suggests a positive correlation between bulk density and moisture content is directly related to the wetter summer months experienced during the study. Increasing bulk density reflects reduced distance between particles and increasing interparticle forces and interactions; a lower bulk density is an indication of increased soil moisture. It is also reasonable that bulk density was negatively correlated to freeze-thaw cycling and positively correlated to soil moisture. Freeze-thaw cycles are only found during the Winter months when bulk density would generally decrease, while high soil moisture is required for freezing-thaw processes to take place (Branson et al., (1996).

Air temperature also explained variance in bulk density both by itself and with GWC. Air temperature alone explained 47 percent of the variance of the average monthly bulk density while air temperature and GWC combined explained 67 percent of the variance in average monthly bulk density. When both air temperature and soil moisture were included as independent variables, the influence they had on the variance within the bulk density measurements was equal: both variables had coefficients of 0.5. Because both coefficients were equal, both independent variables influence the dependent variable, bulk density, equally. Bulk density decreases with decreases in air temperature, again confirming freeze-thaw cycling caused significant disruption of the surface soils.

Table 4.3 Statistically significant regression equations.

Dependent Variable	Equation	P-value	R-Sq (adj.) %	PRESS	Large Residual	Large Influence	Theil-Sen slope	Theil-Sen intercept	Theil-Sen p-value
Kd =	0.854 FTC_30D _{M<0.5}	0.000	70.2	4.169		X	0.9066	-0.1097	0.0197
M_BD =	0.688 M_GMC - 0.439 FTC_10D _{A<1}	0.000	85.5	2.235					
A_BD =	0.627 A_GMC - 0.424 FTC_10D _{A<1}	0.001	72.3	4.977					
A_BD =	0.502 M_GMC + 0.505 AT	0.003	66.5	6.463					
A_BD =	0.721 AT	0.008	47.2	6.523	X		0.7195	0.0428	0.0049

69

Kd = average monthly soil erodibility (cm³/N-s)

M_BD = median monthly bulk density (g/cm³)

A_BD = average monthly bulk density

A_GMC = average monthly gravimetric moisture content (g/g)

M_GMC = median monthly gravimetric moisture content (g/g)

AT = previous month's max daily average air temperature (°C)

FTC_10D_{A<1} = 10 days prior freeze-thaw count when average of sensors <1° C

FTC_30D_{M<0.5} = 30 days prior freeze-thaw count when median of sensors <0.5° C

Chapter 5 Conclusions

The overall goal of this research was to investigate temporal changes in streambank erodibility (K_d) and critical shear stress (τ_c) due to surface weathering. Six experimental reaches along Stroubles Creek near Blacksburg, Virginia, USA were tested monthly from February 2005 to January 2006 for K_d , τ_c , bulk density, and gravimetric water content. The first specific objective for this study was to determine the significance of temporal variability in streambank critical shear stress and erodibility. To investigate the temporal variability of streambank soil characteristics, soil temperature and volumetric moisture content at the bank face were collected every 30 minutes. Precipitation, stream stage, and air temperature were also measured on site. These soil data were then grouped into seasons using cluster analysis based on seasonal soil temperature, seasonal soil moisture, and seasonal air temperature and then analyzed for statistically significant changes from season to season using a nonparametric alternative to ANOVA, the Kruskal-Wallis test, and a nonparametric multiple comparison test. Regression analyses were then conducted to determine if linkages between K_d and τ_c and climatic and soil conditions existed.

During the study, K_d and τ_c ranged from 0.01 and 8.6 cm³/N-s and 0 to 43.3 N/m². During July 2005 and January 2006, K_d and τ_c varied by as much as four and one orders of magnitude, respectively, likely due to the extreme differences in subaerial processes which include dry conditions during the summer and wet conditions with freeze-thaw cycling in the winter. As noted by previous researchers (Hanson, 2001; Wynn and Mostaghimi, 2006b) an inverse relationship between K_d and τ_c existed. Study results showed soil erodibility was impacted by seasonal changes in soil moisture, soil temperature, and air temperature. The median Winter K_d was 1.4 times greater than in Spring/Fall ($p=0.024$) and 75 percent greater than in Summer ($p=0.024$). The median Summer K_d was 37 percent higher than in Spring/Fall ($p=0.024$). Because precipitation during the summer of 2005 was above normal, Summer soil erodibility was likely lower than usual. Seasonal changes in τ_c were not significant ($p=>0.105$). While there were no obvious seasonal trends in τ_c values, the K_d data were highest during the Winter and Summer, when subaerial processes were likely most active. These findings demonstrate quantifiably that soil erodibility is greater in the Winter, lending credence to the observations of Wolman (1959), Twidale (1964), Hooke (1979), Knighton (1973), and Thorne

and Lewin (1979). Significant differences between the sites over the course of the study were not detected (BD by site $p=0.124$; K_d by site $p=0.368$; τ_c by site $p=0.528$), indicating temporal differences in the erosion parameters were more significant than spatial differences.

These results were confirmed by field observations. Streambanks were observed to have very moist, loose outer layers of soil during the winter months. These soil layers were easily removed by the initial five minutes of jet testing or by simply brushing the surface with hand or tool. Behind the surface layer of soil was a denser, undisturbed soil layer which was soft to the touch due to an increase in moisture during the winter months but was not as delicate as the surface soils. In contrast to these observations, the streambank of Stroubles Creek during the summer months was often hard, compact, and covered with desiccation cracks and a dry, loose, sandy soil layer. Beneath both the desiccation cracks was a generally firm, solid soil layer with sufficient structure to withstand physical contact.

The second objective for this study was to evaluate the influence of surface weathering by subaerial processes on streambank critical shear stress and soil erodibility. To investigate these interactions, climatic data were correlated to soil erodibility and critical shear stress using multiple linear regression. Regression analysis showed freeze-thaw cycling was a significant predictor of the variance of soil erodibility. As much as 70 percent of the variance in soil erodibility was explained by freeze-thaw cycling in the 30 days prior to jet testing. No correlation between τ_c and climatic parameters was determined.

Gravimetric water content and freeze-thaw cycles were also shown to explain 85 percent of the variance in bulk density ($p=0.000$). Bulk density was directly related to soil gravimetric water content and inversely related to freeze-thaw cycling during the 10 days prior to jet testing. Bulk density was also positively correlated to air temperature ($R^2=47\%$, $p=0.008$). It is reasonable that bulk density was negatively correlated to freeze-thaw cycling and positively correlated to soil moisture. Freeze-thaw cycles are only found during the Winter months when bulk density would generally decrease, while high soil moisture is required for freezing-thaw processes to take place (Branson et al., (1996). Previous research has shown that both K_d and τ_c were correlated to bulk density (Wynn and Mostaghimi, 2006b). Increasing bulk density reflects reduced distance between particles and increasing interparticle forces and interactions.

These results show significant amounts of variation in the resistance of streambank soils to fluvial erosion can be attributed to subaerial processes, specifically changes in soil moisture

and temperature. These results confirm findings in previous studies Wynn and Mostaghimi (2006b) and Hanson and Simon (2001) that found subaerial processes are major contributors to variations in soil erodibility. The results of this study were likely influenced by the presence of montmorillonite, a high shrink-swell soil, in the streambank. Further research on the influence of subaerial processes on soils with different mineralogy needs to be conducted. One key finding that needs to be investigated further is why critical shear stress did not provide statistically significant relationships to any variable analyzed.

Results of this research have potential implications for streambank modeling and restoration projects that assume constant values for soil erodibility. It will be necessary to evaluate current models and design practices to determine whether there is the potential for error based on changes in soil erodibility over time. Upon further investigation, it may be necessary to insert factors that compensate for the temporal variability that exists in streambank soil erodibility for regions and soils susceptible to degradation due to subaerial processes. Additionally, restoration designs should consider the implications of changing soil erodibility during the year in the design process.

Chapter 6 References Cited

- Allen, P. M., J. Arnold, and E. Jakubowski. 1999. Prediction of stream channel erosion potential. *Environmental and Engineering Geoscience* 5 (3):339-351.
- Arnold, J. G., R. Srinivasan, R. S. Muttiah, and J. R. Williams. 1998. Large area hydrologic modeling and assessment - Part 1: Model development. *Journal of the American Water Resources Association* 34 (1):73-89.
- Arulanandan, K., E. Gillogley, R. Tully. 1980. Development of a quantitative method to predict critical shear stress and rate of erosion of natural undisturbed cohesive soils. *Report GL-80-5*.
- Asare, S., R. Rudra, W. Dickinson, and G. Wall. 1997. Frequency of freeze-thaw cycles, bulk density and saturation effects on soil surface shear and aggregate stability in resisting water erosion. *Canadian Agricultural Engineering* 39 (4):273-279.
- ASTM. 1999. Standard test method for erodibility determination of soil in the field or in the laboratory by the jet index method, No. D 5852-95. 04.08:686-690.
- Benham, B., K. Brannan, T. Dillaha, S. Mostaghimi, R. Wagner, J. Wynn, G. Yagow, and R. Zeckoski. Benthic TMDL for Stroubles Creek in Montgomery County, Virginia. Submitted for Virginia Departments of Environmental Quality, and Conservation and Recreation. Available from <http://www.deq.virginia.gov/tmdl/apptmdls/newrvr/stroub.pdf>.
- Berry, W., N. Rubinstein, B. Melzian, and B. Hill. 2003. The biological effects of suspended and bedded sediment (SABS) in aquatic systems: a review: United States Environmental Protection Agency.
- Blaisdell, F. W., Clayton L. Anderson, George G. Hebaus. 1981. Ultimate dimensions of local scour. *Journal of the Hydraulics Division of the ASCE* 107 (HY3):327-337.
- Boelhouwers, J. C. 1998. Environmental controls on soil frost activity in the Western Cape mountains, South Africa. *Earth Surface Processes and Landforms* 23 (3):211-221.
- Branson, J., D. M. Lawler, and J. W. Glen. 1996. Sediment inclusion events during needle ice growth: A laboratory investigation of the role of soil moisture and temperature fluctuations. *Water Resources Research* 32 (2):459-466.
- Byne, W. 1999. Predicting sediment detachment and channel scour in the process-based planning model ANSWERS-2000, Blacksburg: Virginia Tech, Biological Systems Engineering.
- Chang, H. H. 2002. *Fluvial Processes in River Engineering*. Malabar, Fla.: Krieger Publishing Company.

- Couper, P. 2003. Effects of silt-clay content on the susceptibility of river banks to subaerial erosion. *Geomorphology* 56 (1-2):95-108.
- Couper, P., and I. P. Maddock. 2001. Subaerial river bank erosion processes and their interaction with other bank erosion mechanisms on the river arrow, Warwickshire, UK. *Earth Surface Processes and Landforms* 26 (6):631-646.
- Craig, R. F. 1992. *Soil Mechanics*. London: Chapman and Hall.
- Denef, K., J. Six, R. Merckx, and K. Paustian. 2002. Short-term effects of biological and physical forces on aggregate formation in soils with different clay mineralogy. *Plant and Soil* 246 (2):185-200.
- Dietrich, W., and J. Gallinatti. 1991. Fluvial geomorphology. In *Field Experiments and Measurement Programs in Geomorphology*, edited by O. Slaymaker. Balkema: Rotterdam.
- Edwards, L. M. 1991. The effect of alternate freezing and thawing on aggregate stability and aggregate size distribution of some Prince-Edward-Island soils. *Journal of Soil Science* 42 (2):193-204.
- Ferrick, M. G., and L. W. Gatto. 2005. Quantifying the effect of a freeze-thaw cycle on soil erosion: laboratory experiments. *Earth Surface Processes and Landforms* 30 (10):1305-1326.
- Foster, G. R., L. D. Meyer, and C. A. Onstad. 1977. Erosion equation derived from basic erosion principles. *Transactions of the ASAE* 20 (4):678-682.
- Hanson, G. J. 1990. Surface erodibility of earthen channels at high stresses. Part II - Developing an in situ testing device. *Transactions of the ASAE* 33 (1):132-137.
- Hanson, G. J. 1996. Investigating soil strength and stress-strain indices to characterize erodibility. *Transactions of the ASAE* 39 (3):883-890.
- Hanson, G. J., A. Simon. 2001. Erodibility of cohesive streambeds in the loess area of the midwestern USA. *Hydrological Processes* 15:23-38.
- Hanson, G. J., and K. R. Cook. 2004. Apparatus, test procedures, and analytical methods to measure soil erodibility in situ. *Applied Engineering in Agriculture* 20 (4):455-462.
- Hanson, G. J., K.M. Robinson. 1993. The influence of soil moisture and compaction on spillway erosion. *Transactions of the ASAE* 36 (5):1349-1352.
- Hanson, G. J., K.R. Cook. 1997. Development of excess shear stress parameters for circular jet testing. *ASAE Paper No. 97-2227*.

- Hanson, G. J., K.R. Cook, A. Simon. 1999. Determining erosion resistance of cohesive materials. *Proceedings of the ASCE International Water Resources Engineering Conference, August 8-12, 1999, Seattle, WA.*
- Hanson, G. J., and A. Simon. 2001. Erodibility of cohesive streambeds in the loess area of the midwestern USA. *Hydrological Processes* 15 (1):23-38.
- Helsel, D. R., and R. M. Hirsch. 1993. *Statistical Methods in Water Resources*. Edited by U. S. G. Survey. 69 vols. Vol. 49, *Studies in Environmental Science*. Amsterdam: Elsevier.
- Hollander, M., and D. A. Wolfe. 1973. *Nonparametric Statistical Methods*. New York: Wiley and Sons.
- Hooke, J. M. 1979. An analysis of the processes of river bank erosion. *Journal of Hydrology* 42:39-62.
- Kemper, W. D., and R. C. Rosenau. 1984. Soil cohesion as affected by time and water-content. *Soil Science Society of America Journal* 48 (5):1001-1006.
- Kemper, W. D., R. C. Rosenau, and A. R. Dexter. 1987. Cohesion development in disrupted soils as affected by clay and organic-matter content and temperature. *Soil Science Society of America Journal* 51 (4):860-867.
- Kemper, W. D., T. J. Trout, M. J. Brown, and R. C. Rosenau. 1985. Furrow erosion and water and soil-management. *Transactions of the ASAE* 28 (5):1564-1572.
- Knighton, A. D. 1973. Riverbank erosion in relation to streamflow conditions, River Bollin-Dean, Cheshire. *The East Midland Geographer* 5:416-426.
- Lado, M., M. Ben-Hur, and I. Shainberg. 2004. Soil wetting and texture effects on aggregate stability, seal formation, and erosion. *Soil Science Society of America Journal* 68 (6):1992-1999.
- Langendoen, E. 2000. CONCEPTS - Conservational Channel Evolution and Pollutant Transport System. *Research Report No. 16*.
- Langendoen, E. J., and R. R. Wells. 2004. Concepts- conservational channel evolution and pollution transport system: USDA Agricultural Research Service- National Sedimentation Laboratory.
- Lavelle, W., H.O. Mofjeld. 1987. Do critical stresses for incipient motion and erosion really exist? *Journal of Hydraulic Engineering* 113 (9):370-385.
- Lawler, D. M. 1986. River bank erosion and the influence of frost: A statistical examination. *Transactions of the Institute of British Geographers* 11:227-242.
- Lawler, D. M. 1987. Bank erosion and frost action: an example from South Wales. In *International Geomorphology 1986, Part 1*, edited by V. Gardiner. Chichester: Wiley.

- Lawler, D. M. 1992. Process dominance in bank erosion systems. *Carling, P. and G. E. Petts, eds. Lowland Floodplain Rivers*:117-143.
- Lawler, D. M. 1993. Needle ice processes and sediment mobilization on river banks - the River Ilston, West-Glamorgan, Uk. *Journal of Hydrology* 150 (1):81-114.
- Lawler, D. M. 1995. The impact of scale on the processes of channel-side sediment supply: a conceptual model. *Effects of Scale on Interpretation and Management of Sediment and Water Quality. IAHS Pub.* 226:175-184.
- Lawler, D. M., J. R. Grove, J. S. Couperthwaite, and G. J. L. Leeks. 1999. Downstream change in river bank erosion rates in the Swale-Ouse system, northern England. *Hydrological Processes* 13 (7):977-992.
- Lawler, D. M., C. R. Thorne, and J. M. Hooke. 1997a. Bank erosion and instability. In *Applied Fluvial Geomorphology for River Engineering and Management*, edited by C. R. Thorne, R. D. Hey and M. D. Newson. New York: John Wiley & Sons.
- Lawler, D. M., C. R. Thorne, and J. M. Hooke. 1997b. Bank erosion and instability. In *Applied Fluvial Geomorphology for River Engineering and Management*, edited by C. R. Thorne, R. D. Hey and M. D. Newson. New York: John Wiley and Sons.
- Lehrsch, G. A. 1998. Freeze-thaw cycles increase near-surface aggregate stability. *Soil Science* 163 (1):63-70.
- Lehrsch, G. A., and M. J. Brown. 1995. Furrow erosion and aggregate stability variation in a Portneuf silt loam. *Soil Technology* 7 (4):327-341.
- Lehrsch, G. A., R. E. Sojka, D. L. Carter, and P. M. Jolley. 1991. Freezing effects on aggregate stability affected by texture, mineralogy, and organic-matter. *Soil Science Society of America Journal* 55 (5):1401-1406.
- Matsuoka, N. 1996. Soil moisture variability in relation to diurnal frost heaving on Japanese high mountain slopes. *Permafrost and Periglacial Processes* 7 (2):139-151.
- McBride, M. B. 1994. *Environmental Chemistry of Soils*. New York: Oxford University Press
- Minitab. 2003. *MINITAB Help: Cluster Analysis*, V. 14. State College, PA: Minitab Inc.
- Mostaghimi, S., R. A. Young, A. R. Wilts, and A. L. Kenimer. 1988. Effects of frost action on soil aggregate stability. *Transactions of the ASAE* 31 (2):435-439.
- Osman, A. M., C.R. Thorne. 1988. Riverbank stability analysis I: Theory. *Journal of Hydraulic Engineering* 114:134-150.
- Oztas, T., and F. Fayetorbay. 2003. Effect of freezing and thawing processes on soil aggregate stability. *Catena* 52 (1):1-8.

- Prosser, I. P., A. O. Hughes, and I. D. Rutherford. 2000. Bank erosion of an incised upland channel by subaerial processes: Tasmania, Australia. *Earth Surface Processes and Landforms* 25 (10):1085-1101.
- Schahabi, S., and U. Schwertmann. 1970. Der einfluss von synthetischen eisenoxides auf die aggregation zweier lussbodenhorizonte. *Z. Pflanzenernahr* 125:193-204.
- Sen, P. K. 1968. Estimates of the regression coefficient based on Kendall's tau. *Journal of the American Statistical Association* 63:1379-1389.
- SERCC, S. R. C. C. 2005. Historical Climate Summary, Blacksburg 3 SE: South Carolina Department of Natural Resources, 1000 Assembly Street, Suite 230, Columbia, SC, 29201.
- Simon, A., A. Curini, S. Darby, and E. J. Langendoen. 1999. Streambank mechanics and the role of bank and near-bank processes in incised channels. In *Incised River Channels: Processes, Forms, Engineering, and Management*, edited by S. E. Darby and A. Simon. New York: John Wiley & Sons.
- Six, J., E. T. Elliott, and K. Paustian. 2000. Soil structure and soil organic matter: II. A normalized stability index and the effect of mineralogy. *Soil Science Society of America Journal* 64 (3):1042-1049.
- Summers, J., M. Henderson, and T. Wynn. 2006. Determining the precision of the jet test device. Unpublished data.
- Temple, D. M. 1980. Tractive force design of vegetated channels. *Transactions of the ASAE* 23 (4):884-890.
- Temple, D. M. 1983. Design of grass-lined open channels. *Transactions of the ASAE* 26 (4):1064-1069.
- Temple, D. M. 1985. Stability of grass-lined channels following mowing. *Transactions of the ASAE* 28 (3):750-754.
- Temple, D. M., and S. D. Alspach. 1992. Failure and recovery of a grass channe lining. *Transactions of the ASAE* 35 (1):171-173.
- Theil, H. 1950. A rank-invariant method of linear and polynomial regression analysis. I, II, and III, Proc. Kon. Ned. Akad. v. Wetensch. A. 53:386-392, 521-525, and 1397-1412.
- Thorne, C. R. 1982. Processes and mechanisms for river bank erosion. In *Gravel-bed rivers : fluvial processes, engineering, and management*, edited by R. D. Hey, J. C. Bathurst and C. R. Thorne. New York: John Wiley & Sons Ltd.
- Thorne, C. R. 1990. Effects of vegetation on riverbank erosion and stability. *Thornes, J. B., ed. Vegetation and Erosion: Processes and Environments*:125-144.

- Thorne, C. R., and J. Lewin. 1979. Bank processes, bed material movement and planform development in a meandering river. *Adjustments of the Fluvial System; A Proceedings Volume of the 10th Annual Geomorphology Symposium Series, Beinghamton, NY, September 21, 1979.*:117-137.
- Trimble, S. 1997. Contribution of stream channel erosion to sediment yield from an urbanizing watershed. *Science* 278 (5342):1442-1444.
- Twidale, C. R. 1964. Erosion of an alluvial bank at Birdwood, South Australia. *Annals of Geomorphology* 8:184-211.
- USACE. 1993. *HEC-6: Scour and Deposition in Rivers and Reservoirs, User's Manual, Version 4.1*. Department of the Army, US Army Corps of Engineers, Hydrologic Engineering Center: Alexandria, VA.
- USEPA. 2000. National Water Quality Report to Congress (305(b) report). www.epa.gov/OWOW/305b.
- Van Klaveren, R. W., D.K. McCool. 1998. Erodibility and critical shear of a previously frozen soil. *Transactions of the ASAE* 41 (5):1315-1321.
- Wolman, M. G. 1959. Factors influencing erosion of a cohesive river bank. *American Journal of Science*:204-216.
- Wynn, T. M. 2004. Effects of vegetation on streambank erosion. PhD diss. Blacksburg, VA: Virginia Tech, Department of Biological Systems Engineering
- Wynn, T. M., and S. Mostaghimi. 2006a. Effects of riparian vegetation on streambank subaerial processes in Southwestern Virginia, USA. . *Earth Surface Processes and Landforms* 31 (4):399-413.
- Wynn, T. M., and S. Mostaghimi. 2006b. The effects of vegetation and soil type on streambank erosion, Southwestern Virginia, USA. *Journal of the American Water Resources Association (JAWRA)* 42 (1):69-82.
- Wynn, T. M., S. Mostaghimi, J. A. Burger, A. A. Harpold, M. B. Henderson, and L. A. Henry. 2004. Variation in root density along stream banks. *Journal Of Environmental Quality* 33 (6):2030-2039.
- Zar, J. H. 1999. *Biostatistical Analysis*. 4th ed. Upper Saddle River, N. J.: Prentice Hall.
- Zelazny, L. 2006. Mineralogical Procedure/ Stroubles Creek. Blacksburg, VA, April 27, 2006.

Appendix

Table A-1 Field data collected monthly during jet testing.

Variable	Feb-05	Mar-05	Apr-05	May-05	Jun-05	Jul-05	Aug-05	Sep-05	Oct-05	Nov-05	Dec-05	Jan-06
Average - K_d	1.94	1.32	0.40	0.26	0.39	0.45	0.82	0.50	0.41	0.24	0.97	0.81
Average - τ_c	3.76	6.09	4.59	13.63	12.17	9.25	3.01	5.19	24.56	21.58	10.79	11.97
Median - K_d	1.29	5.55	1.98	12.19	7.20	7.94	1.96	4.19	26.39	22.51	10.26	5.25
Median - τ_c	1.29	5.55	1.98	12.19	7.20	7.94	1.96	4.19	26.39	22.51	10.26	5.25
Average - Bulk Density	1.38	1.23	1.25	1.30	1.32	1.31	1.35	1.35	1.33	1.32	1.23	1.23
Average - Gravimetric MC	0.29	0.42	0.38	0.37	0.36	0.33	0.31	0.29	0.33	0.36	0.35	0.37
Average - Volumetric MC	0.39	0.48	0.45	0.47	0.45	0.43	0.42	0.38	0.43	0.45	0.42	0.45
Median - Bulk Density	1.36	1.31	1.29	1.32	1.35	1.31	1.33	1.37	1.32	1.32	1.27	1.23
Median - Gravimetric MC	0.27	0.32	0.33	0.35	0.31	0.34	0.32	0.27	0.32	0.31	0.35	0.36
Median - Volumetric MC	0.37	0.42	0.43	0.46	0.42	0.44	0.44	0.38	0.44	0.42	0.43	0.45

Table A-2 Monthly soil moisture and temperature data.

Variable	Feb-05	Mar-05	Apr-05	May-05	Jun-05	Jul-05	Aug-05	Sep-05	Oct-05	Nov-05	Dec-05	Jan-06
Average - Bulk Density	1.38	1.23	1.25	1.30	1.32	1.31	1.35	1.35	1.33	1.32	1.23	1.23
Average - Gravimetric MC	0.29	0.42	0.38	0.37	0.36	0.33	0.31	0.29	0.33	0.36	0.35	0.37
Average - Volumetric MC	0.39	0.48	0.45	0.47	0.45	0.43	0.42	0.38	0.43	0.45	0.42	0.45
Median - Bulk Density	1.36	1.31	1.29	1.32	1.35	1.31	1.33	1.37	1.32	1.32	1.27	1.23
Median - Gravimetric MC	0.27	0.32	0.33	0.35	0.31	0.34	0.32	0.27	0.32	0.31	0.35	0.36
Median - Volumetric MC	0.37	0.42	0.43	0.46	0.42	0.44	0.44	0.38	0.44	0.42	0.43	0.45
Average - Daily Air Temp. (°C)	-2.26	2.19	3.87	10.61	13.66	19.44	22.62	22.04	17.44	12.34	6.40	-0.62
Average - Daily Max Air Temp. (°C)	2.89	9.23	11.01	18.55	21.95	26.64	29.22	29.29	27.23	20.06	15.45	5.29
Average - Daily Min. Air Temp. (°C)	-7.38	-3.68	-2.67	2.53	4.99	12.36	17.01	16.17	9.09	6.00	-2.01	-6.00
Maximum - Daily Average Air Temp. (°C)	16.66	9.47	10.80	15.56	19.69	24.24	25.03	24.71	20.68	19.69	17.31	5.19
Maximum - Air Temp. (°C)	18.00	17.20	22.13	26.97	29.33	32.05	34.40	33.70	32.24	29.11	24.50	14.15
Minimum - Daily Average Air Temp. (°C)	-11.45	-3.72	-3.97	2.13	4.66	13.07	19.16	17.62	9.65	2.85	-5.37	-5.46
Minimum - Air Temp. (°C)	-14.70	10.26	15.15	-5.79	-3.07	6.03	11.78	12.56	-0.08	-6.11	10.57	11.90
Total Precipitation (in.)	1.65	4.32	4.31	1.82	3.83	6.34	4.37	0.35	3.50	4.14	2.85	4.12
3 Days Prior - Average Soil Temp. (°C)	5.22	5.71	13.37	17.87		22.45	23.01	20.49	17.78	13.80	3.15	4.48
10 Days Prior - Average Soil Temp. (°C)	5.46	4.42	10.98	14.34	18.28	22.66	23.90	20.34	18.74	13.33	3.86	5.30
30 Days Prior - Average Soil Temp. (°C)	3.72	5.48	8.35	13.20	18.08	22.22	24.23	22.18	20.32	14.30	6.92	4.96
3 Days Prior - Average Volumetric MC	0.29	0.24	0.36	0.31	*	0.39	0.38	0.28	0.34	0.24	0.28	0.31
10 Days Prior - Average Volumetric MC	0.29	0.28	0.38	0.32	0.32	0.40	0.33	0.28	0.30	0.24	0.30	0.29

Table A-2 Cont. Monthly soil moisture and temperature data.

Variable	Feb-05	Mar-05	Apr-05	May-05	Jun-05	Jul-05	Aug-05	Sep-05	Oct-05	Nov-05	Dec-05	Jan-06
30 Days Prior - Average Volumetric MC	0.29	0.29	0.34	0.34	0.33	0.35	0.35	0.31	0.28	0.27	0.29	0.24
3 Days Prior - Average Stage (mV)	0.89	1.22	1.33	0.67	*	1.44	5.89	0.89	1.22	0.67	1.01	*
10 Days Prior - Average Stage (mV)	*	0.90	1.63	0.67	0.94	1.80	2.70	2.77	1.87	0.80	1.31	*
30 Days Prior - Average Stage (mV)	*	*	1.47	0.94	0.97	1.71	1.94	5.81	1.08	0.87	1.49	*
3 Days Prior - Average Air Temp. (°C)	1.32	2.79	13.87	15.46	*	20.76	21.83	16.27	16.68	10.48	-0.83	2.94
10 Days Prior - Average Air Temp. (°C)	1.87	-0.25	10.52	11.03	15.66	21.46	22.04	15.81	16.78	8.95	-1.09	3.18
30 Days Prior - Average Air Temp. (°C)	-1.25	1.99	6.22	10.29	15.26	20.45	22.82	19.60	17.44	10.08	2.67	2.50

Table A-3 Number of freeze-thaw cycles three, 10 and 30 days prior to jet-test for each month using average soil temperatures.

Variable	Feb-05	Mar-05	Apr-05	May-05	Jun-05	Jul-05	Aug-05	Sep-05	Oct-05	Nov-05	Dec-05	Jan-06
3 Days Prior - # of FTC (Average <1.0 °C)	0	1	0	0	0	0	0	0	0	0	1	1
10 Days Prior - # of FTC (Average <1.0 °C)	1	2	0	0	0	0	0	0	0	0	2	3
30 Days Prior - # of FTC (Average <1.0 °C)	10	2	2	0	0	0	0	0	0	0	3	9
3 Days Prior - # of FTC (Average <0.2 °C)	0	1	0	0	0	0	0	0	0	0	0	0
10 Days Prior - # of FTC (Average <0.2 °C)	0	2	0	0	0	0	0	0	0	0	0	1
30 Days Prior - # of FTC (Average <0.2 °C)	4	2	0	0	0	0	0	0	0	0	0	4
3 Days Prior - # of FTC (Average <0.5 °C)	0	1	0	0	0	0	0	0	0	0	0	0
10 Days Prior - # of FTC (Average <0.5 °C)	0	2	0	0	0	0	0	0	0	0	0	1
30 Days Prior - # of FTC (Average <0.5 °C)	6	2	0	0	0	0	0	0	0	0	0	5
3 Days Prior - # of FTC (Average <0.75 °C)	0	1	0	0	0	0	0	0	0	0	0	1
10 Days Prior - # of FTC (Average <0.75 °C)	1	2	0	0	0	0	0	0	0	0	1	2
30 Days Prior - # of FTC (Average <0.75 °C)	9	2	0	0	0	0	0	0	0	0	1	8
3 Days Prior - # of FTC (Average <0 °C)	0	1	0	0	0	0	0	0	0	0	0	0
10 Days Prior - # of FTC (Average <0 °C)	0	2	0	0	0	0	0	0	0	0	0	1
30 Days Prior - # of FTC (Average <0 °C)	2	2	0	0	0	0	0	0	0	0	0	3

Table A-3 Cont. Number of freeze-thaw cycles three, 10 and 30 days prior to jet-test for each month using average soil temperatures.

Variable	Feb-05	Mar-05	Apr-05	May-05	Jun-05	Jul-05	Aug-05	Sep-05	Oct-05	Nov-05	Dec-05	Jan-06
3 Days Prior - # of FTC (Median <1.0 °C)	1	1	0	0	0	0	0	0	0	0	0	1
10 Days Prior - # of FTC (Median <1.0 °C)	2	2	0	0	0	0	0	0	0	0	1	3
30 Days Prior - # of FTC (Median <1.0 °C)	11	5	0	0	0	0	0	0	0	0	1	9
3 Days Prior - # of FTC (Median <0.2 °C)	0	1	0	0	0	0	0	0	0	0	0	0
10 Days Prior - # of FTC (Median <0.2 °C)	0	2	0	0	0	0	0	0	0	0	0	1
30 Days Prior - # of FTC (Median <0.2 °C)	4	2	0	0	0	0	0	0	0	0	0	1
3 Days Prior - # of FTC (Median <0.5 °C)	0	1	0	0	0	0	0	0	0	0	0	0
10 Days Prior - # of FTC (Median <0.5 °C)	0	2	0	0	0	0	0	0	0	0	0	1
30 Days Prior - # of FTC (Median <0.5 °C)	6	2	0	0	0	0	0	0	0	0	0	3
3 Days Prior - # of FTC (Median <0.75 °C)	0	1	0	0	0	0	0	0	0	0	0	2
10 Days Prior - # of FTC (Median <0.75 °C)	1	2	0	0	0	0	0	0	0	0	0	3
30 Days Prior - # of FTC (Median <0.75 °C)	9	3	0	0	0	0	0	0	0	0	0	8
3 Days Prior - # of FTC (Median <0 °C)	0	1	0	0	0	0	0	0	0	0	0	0
10 Days Prior - # of FTC (Median <0 °C)	0	2	0	0	0	0	0	0	0	0	0	1
30 Days Prior - # of FTC (Median <0 °C)	2	2	0	0	0	0	0	0	0	0	0	1

Table A-3 Cont. Number of freeze-thaw cycles three, 10 and 30 days prior to jet-test for each month using average soil temperatures.

Variable			Feb-05	Mar-05	Jun-05	Jul-05	Aug-05	Sep-05	Oct-05	Nov-05	Dec-05	Jan-06
3 Days Prior - # of FTC (Minimum <1.0 °C)	2	4	0	0	0	0	0	0	0	2	1	1
10 Days Prior - # of FTC (Minimum <1.0 °C)	8	8	0	0	0	0	0	0	0	4	4	7
30 Days Prior - # of FTC (Minimum <1.0 °C)	18	20	3	0	0	0	0	0	0	5	8	24
3 Days Prior - # of FTC (Minimum <0.2 °C)	1	3	0	0	0	0	0	0	0	3	0	1
10 Days Prior - # of FTC (Minimum <0.2 °C)	4	6	0	0	0	0	0	0	0	5	1	4
30 Days Prior - # of FTC (Minimum <0.2 °C)	12	11	1	0	0	0	0	0	0	5	4	20
3 Days Prior - # of FTC (Minimum <0.5 °C)	2	3	0	0	0	0	0	0	0	2	1	1
10 Days Prior - # of FTC (Minimum <0.5 °C)	5	6	0	0	0	0	0	0	0	4	2	5
30 Days Prior - # of FTC (Minimum <0.5 °C)	15	12	1	0	0	0	0	0	0	4	5	20
3 Days Prior - # of FTC (Minimum <0.75 °C)	2	3	0	0	0	0	0	0	0	3	1	1
10 Days Prior - # of FTC (Minimum <0.75 °C)	6	7	0	0	0	0	0	0	0	6	3	5
30 Days Prior - # of FTC (Minimum <0.75 °C)	15	15	3	0	0	0	0	0	0	6	7	20
3 Days Prior - # of FTC (Minimum <0 °C)	1	3	0	0	0	0	0	0	0	2	0	0
10 Days Prior - # of FTC (Minimum <0 °C)	4	5	0	0	0	0	0	0	0	4	1	2
30 Days Prior - # of FTC (Minimum <0 °C)	12	9	1	0	0	0	0	0	0	4	3	16

Table A-3 Cont. Number of freeze-thaw cycles three, 10 and 30 days prior to jet-test for each month using average soil temperatures.

Variable			Feb-05	Mar-05	Jun-05	Jul-05	Aug-05	Sep-05	Oct-05	Nov-05	Dec-05	Jan-06
3 Days Prior - # of FTC (Maximum <1.0 °C)	0	0	0	0	0	0	0	0	0	0	0	0
10 Days Prior - # of FTC (Maximum <1.0 °C)	0	0	0	0	0	0	0	0	0	0	0	0
30 Days Prior - # of FTC (Maximum <1.0 °C)	0	0	0	0	0	0	0	0	0	0	0	0
3 Days Prior - # of FTC (Maximum <0.2 °C)	0	0	0	0	0	0	0	0	0	0	0	0
10 Days Prior - # of FTC (Maximum <0.2 °C)	0	0	0	0	0	0	0	0	0	0	0	0
30 Days Prior - # of FTC (Maximum <0.2 °C)	0	0	0	0	0	0	0	0	0	0	0	0
3 Days Prior - # of FTC (Maximum <0.5 °C)	0	0	0	0	0	0	0	0	0	0	0	0
10 Days Prior - # of FTC (Maximum <0.5 °C)	0	0	0	0	0	0	0	0	0	0	0	0
30 Days Prior - # of FTC (Maximum <0.5 °C)	0	0	0	0	0	0	0	0	0	0	0	0
3 Days Prior - # of FTC (Maximum <0.75 °C)	0	0	0	0	0	0	0	0	0	0	0	0
10 Days Prior - # of FTC (Maximum <0.75 °C)	0	0	0	0	0	0	0	0	0	0	0	0
30 Days Prior - # of FTC (Maximum <0.75 °C)	0	0	0	0	0	0	0	0	0	0	0	0
3 Days Prior - # of FTC (Maximum <0 °C)	0	0	0	0	0	0	0	0	0	0	0	0
10 Days Prior - # of FTC (Maximum <0 °C)	0	0	0	0	0	0	0	0	0	0	0	0
30 Days Prior - # of FTC (Maximum <0 °C)	0	0	0	0	0	0	0	0	0	0	0	0

Vita

Marc Henderson was born on January 22, 1981 in Gainesville, FL. From ages 3 till 10, Marc lived in Winter Park, FL. His parents grew tired all the Orlando traffic and hustle and bustle of the big city, so they decided to relocate back to the less chaotic lifestyle found in Gainesville, FL during the summer of 1990. Marc graduated from Eastside High School's International Baccalaureate Program and began his undergraduate studies at his parents' alma mater, the University of Florida, as a third-generation Florida Gator. Marc graduated in December 18, 2003 with a Bachelor of Science degree in Agricultural and Biological Engineering. Gainesville is where Marc still calls home today. On June 5, 2006, Marc will begin work as an Engineer II for the St. Johns River Water Management District in Orlando, FL.